https://doi.org/10.15407/ujpe69.9.642

V. TRUSOVA,[1] I. KARNAUKHOV,[2] A. ZELINSKY,[2] B. BORTS,[2] I. USHAKOV,[2] L. SIDENKO,[1] G. GORBENKO [1]

[1] Department of Medical Physics and Biomedical Nanotechnologies, V.N. Karazin Kharkiv National University
(4, Svobody Sq., Kharkiv 61022, Ukraine; e-mail: valerija.trusova@karazin.ua)
[2] National Science Center "Kharkov Institute of Physics and Technology", Nat. Acad. of Sci. of Ukraine
(1, Akademichna Str., Kahrkiv 61108, Ukraine)

TECHNETIUM-99m: A NANOMATERIAL PERSPECTIVE

The radiolabeling of nanomaterials with technetium-99m (99mTc) has emerged as a promising strategy for integrating the advantages of nanotechnology and nuclear medicine for both diagnostic and therapeutic applications. This comprehensive review aims to provide an in-depth overview of the current state-of-the-art in the radiolabeling of nanomaterials with ^{99m}Tc. The exploration encompasses synthesis methods, labeling mechanisms, biological assessments, physicochemical characterizations, and clinical applications of ^{99m}Tc-labeled nanomaterials. Diverse categories of nanomaterials are addressed, including organic and inorganic nanoparticles, lipid- and protein-based nanosystems, as well as various carbon nanomaterials. Additionally, the review addresses challenges inherent in this evolving field, such as the stability of the radiolabel, potential nanomaterial toxicity, and regulatory considerations. The discussion is concluded by exploring promising future perspectives and potential areas for research development in the realm of ^{99m}Tc-labeled nanomaterials.

Keywords: nanomaterials, theragnostics, technetium, nanomedicine, radiolabeling.

1. Introduction

In the contemporary landscape of medical research and healthcare, the convergence of nuclear medicine and nanotechnology has given rise to a groundbreaking frontier known as nuclear nanomedicine [1]. This nascent field signifies a paradigm shift, amalgamating the accuracy of nuclear medicine with the adaptability and specificity of nanotechnology to inaugurate a new epoch of diagnostic and therapeutic modalities. Nuclear medicine, which was initially focused on macroscopic imaging, has evolved over decades to explore the intricacies of molecular processes within the human body [2]. Utilizing radiotracers and advanced imaging technologies such as single-photon emission computed tomography (SPECT) [1] and positron emission tomography (PET), nuclear medicine facilitates clinicians to examine cellular activities, revealing the molecular etiology of diseases [3]. The evolution of nuclear medicine has paved the way for a more personalized and precise approach to diagnostics and treatment. Concurrently, the field of nanotechnology has experienced a revival, exploiting the unique properties of materials at the nanoscale [4, 5]. Nanomaterials, with their tunable characteristics and multifunctionality, have become the key players in diverse scientific domains. These materials, often smaller than 100 nanometers, exhibit distinctive physical and chemical properties, rendering them candidates for targeted drug delivery, imaging enhancement, and theranostic applications.

The integration of nuclear medicine and nanotechnology, encapsulated in the term nuclear nanomedicine, represents a synergy that leverages the strengths of both fields. Radiolabeled nanomaterials, tailored for specific clinical applications, bring a new level of precision to molecular imaging and therapeutic interventions [6–8]. This integration holds the

[1] For the list of abbreviations, see Appendix.

Citation: Trusova V., Karnaukhov I., Zelinsky A., Borts B., Ushakov I., Sidenko L., Gorbenko G. Technetium-99m: a nanomaterial perspective. *Ukr. J. Phys.* **69**, No. 9, 642 (2024). https://doi.org/10.15407/ujpe69.9.642.

promise of overcoming traditional limitations in sensitivity, specificity, and therapeutic efficacy, thereby revolutionizing the landscape of medical interventions. At the core of nuclear nanomedicine lies the concept of theranostics, embodying the dual functionality of diagnostics and therapeutics within a single platform [9]. Theranostic agents, often composed of radiolabeled nanomaterials, provide a versatile toolkit for clinicians. They enable not only the non-invasive visualization of molecular processes, but also the targeted delivery of therapeutic payloads to specific sites, fostering a more personalized and effective treatment paradigm [10–12].

A significant number of radionuclides have been integrated into various nanoplatforms, ushering in opportunities for targeted molecular imaging, early disease detection, and the development of personalized treatment strategies [13–18]. Among them, technetium-99m (^{99m}Tc) is renowned as a radiopharmaceutical stalwart that boasts ideal nuclear characteristics rendering it particularly suited for a spectrum of imaging applications [19–22]. Its relatively short half-life of approximately six hours aligns favorably with diagnostic imaging needs, ensuring timely data acquisition without subjecting patients to prolonged radiation exposure. This optimal half-life is crucial for scenarios demanding rapid imaging, providing real-time insights into intricate biological processes. One of the distinctive advantages of technetium lies in its versatility across various imaging modalities. The gamma emission of ^{99m}Tc extends its applicability beyond SPECT, enabling multimodal imaging that enhances diagnostic precision. This adaptability is pivotal in widening the diagnostic scope and addressing diverse clinical requirements [22]. The widespread availability of technetium-99m further solidifies its position as a radionuclide of choice. The emissions profile of ^{99m}Tc, characterized by low-energy gamma rays, contributes to reduced radiation exposure for both patients and medical personnel. This safety consideration enhances the overall profile of diagnostic procedures, aligning with contemporary healthcare standards. Moreover, the chemical properties of ^{99m}Tc facilitate straightforward labeling procedures with various nanomaterials. This compatibility ensures efficient and reliable integration, preserving the structural and functional integrity of the nanocarriers. The seamless incorporation of technetium into nanomaterials further underscores its position as a preferred choice for nuclear medicine applications.

The present contribution initiates an in-depth examination of the intricate molecular processes involved in radiolabeling nanomaterials with technetium-99m, revealing its substantial potential for disease diagnosis, treatment efficacy monitoring, and the formulation of personalized therapeutic strategies. Our exploration will navigate the foundational principles that underscore this approach, scrutinizing the complexities inherent in radiolabeling procedures. Additionally, we will survey the diverse applications that extend across various medical domains such as oncology, cardiology, neurology, and far beyond.

2. Chemistry and Radiochemistry of ^{99m}Tc

Over the past four decades, technetium-99m (^{99m}Tc)-based radiopharmaceuticals have become indispensable tools in the diagnosis of a variety of diseases. Currently, the field has an impressive diversity of over a hundred ^{99m}Tc-based compounds for the use in nuclear medicine, which together account for nearly 80% of routine clinical procedures in nuclear medicine services [21]. The widespread use of ^{99m}Tc radiopharmaceuticals can be attributed to the excellent nuclear decay properties of this isotope. These include a physical half-life of 6.03 h and the emission of pure γ-radiation at an energy level of 140 keV. A pivotal enabler of the extensive usage of ^{99m}Tc-based radiopharmaceuticals is the ^{99m}Mo/^{99m}Tc generator, which serves multiple crucial functions [22]. First, it facilitates distribution to geographically remote medical facilities, ensuring accessibility to these vital diagnostic tools. Second, it allows for the transformation of the radiometal into various states of oxidation, expanding the scope of coordination chemistry and enabling the creation of diverse radiopharmaceuticals. In addition, the direct reconstitution of the lyophilized kit simplifies the preparation process, making ^{99m}Tc-based radiopharmaceuticals very convenient for clinical application [23]. Furthermore, these drugs have a very low incidence of side effects compared to other contrast agents, thereby increasing their safety in medical practice.

One of the most compelling aspects of metallic radionuclides such as ^{99m}Tc is their versatility in forming complexes with a variety of ligands, including biological macromolecules, monoclonal antibodies, small peptides, nanoparticles, *etc.* This inherent flexibility

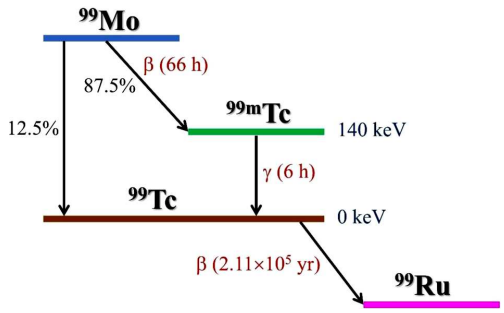

Fig. 1. Production of technetium-99m

enables researchers and clinicians to create a variety of complexes targeting specific diagnostic or therapeutic targets. Essentially, the ability of ^{99m}Tc to engage in coordination chemistry with such a variety of ligands constitutes a paramount advantage, fueling ongoing advancements in radiopharmaceutical development.

Technetium, designated as element 43, came into scientific awareness in 1937, when Perrier and Segrè found it in a sample of molybdenum that had undergone irradiation by deuterons [24]. This major discovery marked the first instance in which an element, previously unknown, had been artificially synthesized. The name "technetium" comes from the Greek "technetos" meaning "artificial". Our understanding of technetium was further advanced in 1939, when Seaborg and Segrè observed the transformation of molybdenum-98 upon slow neutron irradiation to form ^{99}Tc through the decay of the metastable isomer ^{99m}Tc [26]. Over time, researchers discovered a total of 21 isotopes of technetium, ranging from ^{90}Tc to ^{110}Tc. Among these isotopes, ^{110}Tc has the shortest half-life of only 0.86 sec, while ^{97}Tc has the longest half-life of approximately 2.6 million years. It is important to note that all technetium isotopes are radioactive in nature.

^{99m}Tc is classified as a metastable nuclear isomer, as denoted by the "m" following the mass number. Nuclear isomers have nuclei in a higher energy state than the ground state [26]. Figure 1 shows the decay scheme for ^{99}Mo with 12.5% of the decays through beta emission to yield ^{99}Tc, and, in the remaining 87.5% of the decays, to produce ^{99m}Tc. Approximately 13% of the ^{99m}Tc decays result in the creation of the long half-life isotope ^{99}Tc, with a half-life of 2.11×10^5 years. The decay of ^{99m}Tc to ^{99}Tc is accompanied by the emission of gamma radiation, while the subsequent decay of ^{99}Tc to ^{99}Ru involves the emission of a β-particle.

Generally, pertechnetate, $[^{99m}TcO_4]^-$, is considered the most convenient starting material for the synthesis of ^{99m}Tc-based compounds. This is mainly so, because its direct obtention from the ^{99}Mo/^{99m}Tc generator [27]. To introduce ^{99m}Tc into biomolecules, TcO_4^- must be reduced from its initial oxidation state +7 to a lower oxidation state [28]. Key oxidation states for the development of ^{99m}Tc-based radiopharmaceuticals corresponds to +5, +3 and +1 [29]. The resulted oxidation state of ^{99m}Tc depends on various factors, including the type and proportion of the reducing agent, the presence of available ligands, oxygen levels, and the specific reaction conditions employed during synthesis. In view of its short half-life (∼6 h), it is highly advisable to complete the synthesis of radiopharmaceuticals within a 30-minute timeframe. Maintaining these conditions is crucial, since the injection of a mixture of different ^{99m}Tc species can weaken organ specificity and increase + radiation dose administered to patients [30]. Nevertheless, despite the short half-life, ^{99m}Tc provides sufficient time for the preparation of radiopharmaceuticals and the acquisition of valuable images without imposing an undue radiation burden on the patient. Moreover, the monochromatic 140 keV photons emitted by ^{99m}Tc are easily captured and quantified, resulting in high spatial resolution images [31].

Due to its favorable nuclear properties and versatility, technetium-99m is widely used in various imaging techniques in nuclear medicine, particularly in single-photon emission computed tomography (SPECT). SPECT is a non-invasive nuclear imaging technique used in medical diagnostics to examine the functional activities of various organs within the body [32]. It provides three-dimensional images, allowing gaining insights into the function, blood flow, and metabolic processes of organs and tissues. SPECT imaging is particularly valuable in the diagnosis and management of various diseases and conditions. In brief, the procedure of SPECT imaging involves the following algorithm (Fig. 2). Before the SPECT scan, the patient is injected with a radiopharmaceutical which contains a radioactive tracer, ^{99m}Tc, attached to a carrier molecule that targets specific tissues or organs [33]. The tracer is designed to accumulate in the area of interest, specifically, heart, brain, bones, or other organs.

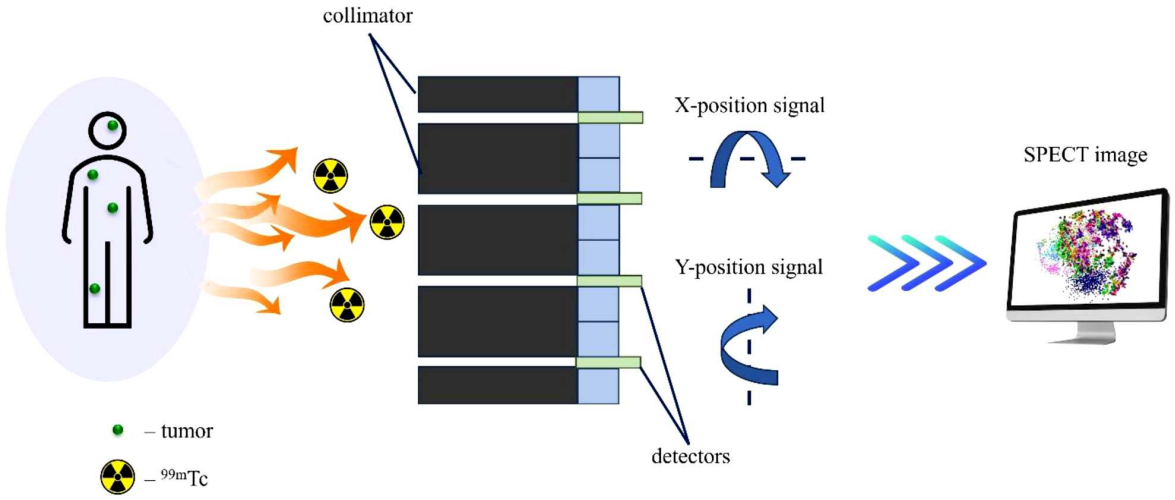

Fig. 2. Principal scheme of SPECT scanning

It emits γ-rays that can be detected by a gamma camera. The radiopharmaceutical circulates through the bloodstream and accumulates in the targeted tissue or organ. The distribution depends on the specific properties of the radiotracer and the physiological processes of the organism. Once the radiopharmaceutical has had sufficient time to accumulate in the targeted area, the patient is positioned on a scanning table. A gamma camera, which can rotate around the patient, is used to detect the gamma rays emitted by the radiopharmaceutical. The camera captures multiple images from different angles. These images are subsequently reconstructed, enabling the visualization of the distribution and concentration of the radiopharmaceutical within the body. Finally, the careful analysis of the generated SPECT images allows precise personalized diagnostics.

Table 1 provides a consolidated overview of ^{99m}Tc radiopharmaceuticals, showcasing their respective applications, chelators, and target localizations [34–36]. The inclusion of an extensive array of radiopharmaceuticals serves to illustrate the versatility and continued evolution of ^{99m}Tc-based compounds in the field of nuclear medicine.

Choosing the appropriate radiopharmaceuticals based on ^{99m}Tc is crucial in order to achieve the accurate and focused imaging for various medical purposes. As the field continues to evolve, ongoing research and advancements in radiopharmaceutical development are anticipated, further enriching the array of diagnostic tools based on ^{99m}Tc.

3. General Characteristics and Classification of Nanomaterials Used in Nuclear Medicine

In the domain of nuclear medicine, nanomaterials have emerged as pivotal entities, introducing a paradigm shift in diagnostic imaging, targeted therapies, and drug delivery [37, 38]. Their unique characteristics, rooted in their nano-sized dimensions and tailored physicochemical properties, render them indispensable tools in the intricate landscape of nuclear medicine applications. Nanomaterials, typically falling within a size range of 1 to 100 nanometers, exhibit distinctive properties arising from their quantum scale. This size regime imparts nanomaterials with large surface area-to-volume ratios, fostering enhanced interactions at the molecular and cellular levels. One of their key attributes lies in the tunability of their surface properties, allowing for modifications that enhance biocompatibility, stability, and the ability to bind specific biomolecules [39].

Nanomaterials can be sorted into different groups based on their dimensionality, morphology, state, and chemical composition. Despite the different categories of NMs, proposed in literature, the generally accepted classification relies on the chemical origin of their nature [40]. In this regard, nanomaterials can be categorized into three primary groups: i) inorganic nanomaterials (noble and magnetic metals, non-metals); ii) organic bionanomaterials (polymers and lipids); iii) carbon-based nanomaterials [41].

Table 1. **^{99m}Tc-based radiopharmaceuticals commonly used in nuclear medicine**

Radiopharmaceutical	Purpose/Application	Target/Localization	Diagnostic Modality
^{99m}Tc-SestaMIBI	Cardiac imaging (myocardial perfusion)	Heart (myocardium)	SPECT
^{99m}Tc-Tetrofosmin	Cardiac imaging (myocardial perfusion)	Heart (myocardium)	SPECT
^{99m}Tc-Pentetate (DTPA)	Renal imaging (glomerular filtration), ventilation imaging (pulmonary inhalation)	Kidneys, lungs (for pulmonary ventilation studies)	Dynamic scintigraphy, planar imaging
^{99m}Tc-Mertiatide (MAG3)	Renal imaging (renal function, renography)	Kidneys	Dynamic scintigraphy
^{99m}Tc-hepatobiliary iminodiacetic acid (HIDA)	Hepatobiliary imaging	Liver, biliary tract	Planar imaging
^{99m}Tc-methylene diphosphonate (MDP)	Bone scintigraphy	Bones (for detection of bone abnormalities)	" "
^{99m}Tc-macroaggregated albumin (MAA)	Lung perfusion imaging	Lungs (for pulmonary perfusion studies)	" "
^{99m}Tc-Exametazime (HMPAO)	Brain imaging (cerebral blood perfusion)	Brain (for cerebral flow studies)	SPECT
^{99m}Tc-sulfur colloid	Liver and spleen imaging	Liver, spleen	Planar imaging
^{99m}Tc-red blood cells	Blood pool imaging	Cardiovascular system	" "
^{99m}Tc-Disofenin	Hepatobiliary imaging	Liver, biliary tract	" "
^{99m}Tc-Pyrophosphate	Cardiac imaging (myocardial infarction)	Heart (for detection of myocardial infarction)	" "
^{99m}Tc-metaiodobenzylguanidine (MIBG)	Neuroendocrine tumor imaging	Adrenal glands, sympathetic nervous tissue	SPECT
^{99m}Tc-Tilmanocept	Sentinel lymph node mapping	Lymph nodes	Planar imaging
^{99m}Tc-radiolabeled antibodies	Targeted cancer imaging	Specific cancer cells	SPECT/PET

Each class of NMs is characterized by its own set of pros and cons, and the choice of a suitable nanomaterial, radioisotope, and radiolabeling approach is dictated by the specific medical purpose. Accordingly, inorganic nanomaterials exhibit the high stability and durability, high surface area, and unique optical and catalytic properties [42]. These make them valuable for medical imaging and radiolabeling. In the meantime, inorganic NMs may require additional biocompatible coatings, and have the potential for toxicity, which necessitates careful consideration of their utilization in biomedical applications. The appeal of organic nanomaterials lies in their unique attributes such as structural, mechanical, and functional diversity, high biocompatibility and biodegradability, minimal invasiveness, and versatility for encapsulating and delivering both radiolabels and therapeutic agents. In addition, organic NMs can be tailored for controlled radiotracer delivery, enhancing thereby precision of diagnostic and treatment [43].

While inorganic nanomaterials typically result from the precipitation of inorganic salts or the reduction of metallic ions, organic NMs consist of self-organized organic molecules such as lipids, proteins or polymers, held together by relatively weak interactions, with the notable exception of dendrimers, which represent the single molecules [44]. Due to the nature of these interactions, organic nanomaterials are dynamic systems, which can merge, expand, and form a larger architectures. Unlike inorganic nanomaterials, which can be as diminutive as a few atoms, the size of some or-

ganic NMs is constrained by the dimensions of their molecular constituents.

A special attention should be given also to carbon-based structures due to their fascinating physicochemical properties. Accordingly, carbon nanomaterials (CNMs) can exhibit various morphologies, spanning from zero to three dimensions. The carbon atoms within CNMs can exhibit different hybridization states, such as sp^2 or sp^3 hybridization [45, 46]. Within this diverse family, various structures are encompassed, ranging from zero-dimensional examples like carbon quantum dots (CQDs) and fullerenes, to one-dimensional forms such as carbon nanotubes (CNTs) and carbon nanofibers (CNFs), two-dimensional sheets like graphene, and even three-dimensional structures like carbon nanodiamonds. Carbon nanomaterials (CNMs) have demonstrated impressive performance across a wide spectrum of applications, spanning from biomedicine to the automotive industry [47, 48].

4. Current Protocols for ^{99m}Tc Radiolabeling of NMs

The first step in design of modern ^{99m}Tc-based radiopharmaceuticals relies on chemical conjugation of technetium complexes to a desired nanomaterial. This stage is known as the labeling procedure. In the process of choosing a specific NM to treat a clinically significant disease, by determining the labeling method. The process of labeling can significantly shape the biomolecule's behavior within a biological context, thereby influencing the ultimate quality of the image and the success of the diagnostic procedure. Unlike the conventional labeling using PET radionuclides such as ^{11}C, ^{18}F, and ^{123}I, SPECT employs a more intricate label, which comprises a multicomponent system. This system is comprised of a transition metal center and various inherently linked groups, collectively forming the "core" (Fig. 3). These metal fragments are chemical patterns defined by a specific arrangement of atoms linked to the metal center, shaping the creation of diverse coordination complexes and molecular geometries.

4.1. Labeling with ^{99m}Tc-oxo-core

The most widely used technetium core, applied in bio/nanopharmaceutics, is the ^{99m}Tc-oxo moiety, $[TcO(H_2O)_4]^{3+}$ [49]. Typically, complexes built upon this core exhibit pentacoordination and adopt a square pyramidal geometry, with the oxo-group involved in π-bonding occupying the apex position. Six-coordinated technetium-oxo compounds are relatively rare, primarily due to the strong trans influence of the oxo-group.

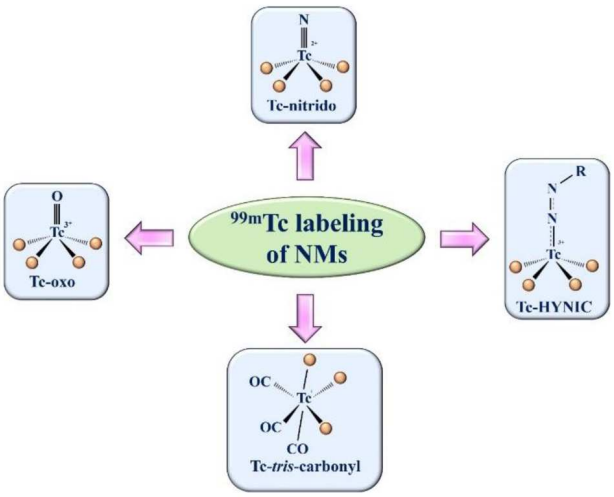

Fig. 3. Main approaches for radiolabeling of nanomaterials with ^{99m}Tc

The stability and integrity of oxo-group are maintained through the contribution of π- and σ-donating atoms derived from amino, amido, and thiolate ligands, as well as tetradentate ligands falling within the $N_{4-x}S_x$ coordination category [50]. These ligands demonstrate a remarkable ability to create ^{99m}Tc-oxo complexes that are considerably more stable in comparison to those formed by bidentate ligands. These compounds can be synthesized either through the direct reduction of the ^{99m}Tc-pertechnetate anion in the presence of tin chloride, which is a common initial step in the preparation of traditional ^{99m}Tc-radiopharmaceuticals, or through a ligand exchange reaction with [^{99m}Tc]Tc-glucoheptonate [51].

4.2. Nitrido technetium-99m core for radiolabeling

Technetium nitrido complexes, $[TcN(H_2O)_4]^{2+}$ are identifiable by their distinctive [Tc≡N] multiple-bond unit. The nitrido nitrogen atom demonstrates robust π-electron donating capabilities. In cases where it functions as a terminal ligand, the [Tc≡N] moiety exhibits a formal bond order of three [52]. This triple bond arises from the formation of one σ-bond and

two π-bonds, with the latter emerging from the interaction between the occupied p orbitals of nitrogen and the unoccupied $4d$ orbitals of the metal that exhibit the required symmetry. In contrast to the synthesis of metal oxo-complexes, where a residual oxygen atom remains bonded to the metal following the reduction of $[^{99m}\mathrm{Tc}]\mathrm{NaTcO_4}$ in an aqueous solution, the generation of the nitrido moiety necessitates a reaction between pertechnetate and a donor of nitrido nitrogen atoms in the presence of a reducing agent [53]. The process of labeling with ^{99m}Tc-nitrido core is straightforward, allowing for a significant modifications, while keeping the central core intact. The ligands attached to biomolecules are straightforward and readily accessible in the commercial market. One challenge, however, is the use of air-sensitive and potentially harmful phosphines [54].

4.3. HYNIC labeling

HYNIC (2-hydrazinonicotinic acid) was one of the most popular and effective bifunctional chelators used for radiolabeling with ^{99m}Tc [55]. This labeling approach is used preferentially for the labeling of the peptide/protein- and nucleic acid-based nanomaterials [56]. HYNIC is typically attached to biomolecules through the formation of an amide bond. This bond is established by reacting the amine side chains within the biomolecule with an active ester derivative of HYNIC, such as the N-hydroxysuccinimide or tetrafluorophenyl esters [57]. Given that HYNIC can only coordinate to a metal through a maximum of two donor groups (pyridyl nitrogen and hydrazine nitrogen), it is incapable of fully occupying the pyramidal or octahedral coordination of technetium. Consequently, additional co-ligands are needed to complete the coordination sphere. The need for co-ligands introduces a substantial level of flexibility in designing and applying this dual-purpose chelating system. However, it also brings about a significant degree of uncertainty regarding the configuration of the coordination sphere, and it is optimization to create radiopharmaceuticals that offer the utmost convenience, efficient labeling, structural uniformity, *in vivo* stability, and targeted properties.

4.4. Conjugation through ^{99m}Tc tris-carbonyl nucleus

Complexes involving a low-oxidation state technetium, particularly those with the metal in the +1 oxidation state, represented by the core $[^{99m}\mathrm{Tc(CO)3}]^+$, have garnered considerable interest. This significance arises from the compact size of these complexes and their low-spin electron configuration (d^6), which imparts excellent thermodynamic and kinetic stability. In addition, it contains three fixed CO ligands in comparison to oxygen or nitrogen in $[\mathrm{Tc{=}O}]^{3+}$ or $[\mathrm{Tc{\equiv}N}]^{2+}$ moieties, respectively [58]. Furthermore, the remaining coordination sites are occupied by three water molecules. These water molecules can be replaced by a large variety of ligands that have electron donors in their structure, such as amines, imines, thioethers, thiols, carboxylates, phosphates and phosphonates. Nonetheless, the $[^{99m}\mathrm{Tc(CO)3}]^+$ core exhibits a preference for coordinating with amine groups rather than carboxylate groups [31]. Typically, bidentate chelators form stable $^{99m}\mathrm{Tc}^{+1}$ complexes in solution, but they may display a relatively low stability in vivo. This phenomenon can be attributed to the higher lipophilicity of cationic ^{99m}Tc radiocomplexes, a characteristic that is notably influenced by the presence of bidentate chelators. The complexes based on ^{99m}Tc *tris*-carbonyl are exceptionally resilient and, generally, do not undergo decomposition in serum or within the living organism.

5. ^{99m}Tc Conjugation to Inorganic Nanomaterials

In the field of contemporary material nanoscience, inorganic NMs are emerging as innovative therapeutic and imaging assays, thanks to their unique physical attributes, including size-dependent optical, magnetic, electronic, and catalytic properties [59–62]. These nanomaterials are characterized by their high stability, substantial surface area, adjustable compositions, diverse physicochemical versatility, and specific biological functionalities [42, 43].

Table 2 lists the selection of ^{99m}Tc-labeled nanomaterials with the accent on their purpose, radiolabeling methods, and associated imaging or therapeutic modalities. Some of these examples will be discussed within the present review, others are given for illustration.

The above table encapsulates a spectrum of nanomaterials radiolabeled with technetium-99m, emphasizing their versatility in addressing challenges in biomedicine. Each example reflects the ongoing efforts to harness the unique properties of nanomaterials for precise diagnostics and targeted ther-

Table 2. **Nanomaterials radiolabeled with ^{99m}Tc and their clinical applications**

Nanomaterial	Radiolabeling method	Clinical applications	Imaging/Therapeutic modality	References
Gold nanoparticles	Direct labeling, thiol-based linkage	Cancer theranostics, photothermal cancer therapy	SPECT/CT imaging, photothermal therapy	[63, 64]
Iron oxide nanoparticles	Direct labeling, chelation with DTPA	Contrast agent for MRI, detection of liver lesions	SPECT/MRI imaging	[20, 65]
Silica nanoparticles	Direct labeling, chelation with MAG3	Drug delivery and imaging	SPECT imaging, drug delivery	[66, 67]
Magnetic nanoparticles	Direct labeling, thiol-based linkage	Cancer imaging, imaging of cardiovascular diseases and inflammation, magnetic hyperthermia for tumor treatment	SPECT/CT imaging, magnetic hyperthermia	[68, 69]
Lipid nanoparticles	Direct labeling, chelation with HYNIC	Targeted drug delivery, imaging of lipid-based therapies	SPECT imaging, drug delivery	[70, 71]
Liposomes	Direct labeling, chelation with HYNIC	Cancer theranostics, drug delivery to tumors, non-invasive imaging of drug biodistribution	SPECT imaging, drug delivery	[72, 73]
Protein-based nanoparticles	Direct labeling, covalent bonding with HYNIC	Targeted drug delivery, imaging-guided therapy	SPECT imaging, drug delivery	[20, 74]
Polymeric nanoparticles	Direct labeling, covalent bonding with HYNIC	Targeted drug delivery, imaging-guided cancer therapy, detection of inflammation and bacterial infections	SPECT imaging, drug delivery	[75, 76]
Polymeric micelles	Direct labeling, covalent bonding with HYNIC	Targeted drug delivery, imaging-guided cancer therapy, detection of inflammation and bacterial infections	SPECT imaging, drug delivery	[77]
Quantum dots	Direct labeling, surface functionalization with HYNIC	Cellular imaging, sentinel lymph node mapping, detection of metastatic cancer cells	SPECT imaging, multimodal imaging	[78, 79]
Carbon nanotubes	Direct labeling, covalent bonding with HYNIC	Cancer imaging, photothermal therapy for tumor ablation	SPECT/CT imaging, photothermal therapy	[20, 45]
Dendrimers	Direct labeling, chelation with MAG3	Cancer imaging, targeted drug delivery to specific cells	SPECT imaging, drug delivery	[80, 81]
Graphene oxide nanosheets	Direct labeling, thiol-based linkage	Multimodal imaging, targeted drug delivery	SPECT imaging, drug delivery, multimodal imaging	[82, 83]
Nanogels	Direct labeling, covalent bonding with HYNIC	Targeted drug delivery, imaging of inflamed tissues	SPECT imaging, drug delivery	[84, 85]

apeutic interventions. It is essential to acknowledge that this table is not exhaustive, and the dynamic nature of nanomedicine continually introduces new developments.

5.1. ^{99m}Tc radiolabeling of noble metal nanomaterials

Gold nanomaterials (AuNMs) have garnered growing attention as imaging and therapeutic agents due to their biocompatibility, stability, and optoelectronic properties. Beyond their applications in optical imaging, radiosensitization, and photothermal therapy, these nanoparticles are capable of carrying medically relevant radionuclides. This feature extends their utility to nuclear medical imaging and radionuclide therapy. Functionalized gold nanoparticles (AuNPs) are high-contrast agents for hybrid imaging techniques, such as SPECT alone or combined with

CT [32]. Radiolabeled AuNMs have received a considerable attention in the SPECT imaging due to their high sensitivity, the capability for deep tissue penetration, and their translational potential for clinical use. Various radionuclides, including ^{125}I, ^{111}In, ^{131}I, and ^{99m}Tc, have been successfully attached to functionalized AuNPs [86-88]. Furthermore, the dual incorporation of radionuclides, such as ^{125}I and ^{111}In, has been employed to create multimodal probes for SPECT bioimaging.

A good wealth of reports present in literature describes the benefits of ^{99m}Tc conjugation to AuNMs [90–92]. Specifically, a multimeric platform composed of ^{99m}Tc-tagged gold NPs of 20 nm in size, conjugated to HYNIC-Gly-Gly-Cys-NH_2 and cyclic [Arg-Gly-Asp-Phe-Lys(Cys)] peptides as novel promising radiopharmaceutical for imaging of the $\alpha_\nu\beta_3$ integrin expression, a membrane receptor, playing a key role in tumor angiogenesis and metastasis [89]. The obtained nanoconjugate was comprehensively characterized by a set of analytical tools, including TEM, FTIR, UV-vis, and Raman spectroscopy. ^{99m}Tc-labeled AuNPs linked to the peptides, characterized by $\geq 94\%$ of radiochemical purity, showed an extreme stability in human serum and profound and specific $\alpha_\nu\beta_3$-positive tumor uptake during the in vivo studies.

A different methodological approach was used in the work [90] by Xing *et al.* By combining various chemical protocols, the authors synthesized, characterized and utilized ^{99m}Tc-labeled gold nanoparticles, entrapped into poly(amido-amine) dendrimers. In brief, ^{99m}Tc radiolabeling of functionalized AuNPs was conducted via the procedure of 4,7,10-tetraazacyclododecane-1,4,7,10-tetraacetic acid chelation [91]. The quantitative analysis of SPECT images recorded at the ^{99m}Tc dose of 400 μCi/ml showed that the designed radiolabeled nanosystems displayed excellent stability and cytocompatibility over the wide concentration range both *in vitro* and *in vivo* studies and revealed their great potential in identifying early steps of apoptosis of the cancer cells.

A multifunctional system containing ^{99m}Tc-labeled mannose-functionalized Au nanoparticles was developed as nanoprobe for the sentinel lymph node detection [86]. The ^{99m}Tc radiolabeling was performed via HYNIC assay. The results of the SPECT imaging demonstrated that ^{99m}Tc-radiolabeled AuNPs exhibit the ability to track and accumulate in lymph nodes in a way, similar to commercially available ^{99m}Tc-sulfur colloid. The latter is a commonly employed clinical agent for sentinel lymph node detection [92]. These encouraging findings give support to the notion that ^{99m}Tc-AuNPs-mannose could serve as a valuable SPECT contrast agent for lymphatic mapping.

Santos *et al.* obtained ^{99m}Tc-labeled silver tungstate nanoparticles and evaluated their potential as a new tool for tumor identification and uptake [93]. The synthesis of NPs was performed through microwave-assisted hydrothermal procedure, and radiolabeling with ^{99m}Tc was implemented via the standard protocol of technetium reduction achieving, thereby, the degree of labeling exceeding 95%. The Raman spectroscopy and X-ray diffractometry data provided insights into the structural organization of compounds at both long and short-range scales. Additionally, the examination of the polydispersity index (PDI) and zeta potential indicated that silver tungstate forms a homogeneous and stable suspension in an aqueous medium. Biodistribution studies revealed that the nanoparticles exhibited a preference for accumulating in tumor tissue over normal tissues, presumably due to the enhanced permeation and retention effect.

Successful formulation of gold nanoparticles with ^{99m}Tc and doxorubicin (DOX) for the targeted delivery of radiopharmaceuticals to the tumor cells was reported in [94]. Accordingly, loading of radioactive ^{99m}Tc with DOX allows creation of multifunctional Au-based nanoplatform suitable for simultaneous biodistribution studies and identification of early steps of tumor cell apoptosis. Based on a set of studies of in vitro and in vitro stabilities, the authors concluded that radiolabeling of AuNPs with preformed ^{99m}Tc-DOX complexes results in higher potential of this composite radiopharmaceutical delivery platform as compared to sequential addition of ^{99m}Tc and DOX solutions.

Analogous approach has been applied by El-Safoury *et al.* in [95]. Specifically, the authors synthesized a novel nanoradiopharmaceutical utilizing gold nanoparticles loaded with ^{99m}Tc and chemotherapy drug methotrexate. The final drug delivery nanocontainers were characterized by uniform size distribution (20.3 nm), polydispersity index less than 0.5 and zeta-potential of *ca.* –17.6 mV. The functionalized AuNPs showed high anticancer activity against MCF-7 breast cancer cells, and high tumor uptake in solid tumor bearing mice. The remark-

able tumor-targeting precision and selectivity of integrated ^{99m}Tc-Mex-AuNPs, coupled with increased cytotoxicity, position them as a promising theranostic nanoradiopharmaceuticals offering dual utility for both tumor diagnostics and treatment.

The radiolabeling of neat and dextran-coated silver nanoparticles (AgNPs and dextran-AgNPs, respectively) with ^{99m}Tc was performed by Ashraf *et al.* [96] to monitor their uptake in various organs under SPECT γ-camera. Dynamic imaging was employed to assess the quantification and biodistribution of ^{99m}Tc-labeled nanoparticles in primary organs, including the liver, stomach, kidneys, and bladder. Neat AgNPs exhibited high liver uptake, while nanoparticle functionalization with dextran resulted in delayed recognition and uptake by the reticuloendothelial system and prolonged retention in the blood pool. Notably, the clearance of nanoparticles from various organs was rapid, ultimately leading to a more extended relative blood pool image. These findings suggest that dextran-coated AgNPs can persist in the bloodstream for an extended duration.

5.2. The advances in ^{99m}Tc radiolabeling of iron nanomaterials

In the past ten years, radiolabeled iron nanomaterials have emerged as promising contrast agents suitable for dual-modality imaging, including PET/MRI and SPECT/MRI. This fusion of PET (or SPECT) with MRI provides synergistic benefits, enabling non-invasive, high-sensitivity, high-resolution, and quantitative imaging [97]. Such capabilities are well-suited for the early detection of a range of diseases, including cancer. The labeling of iron nanoparticles relies on a fact that reduced ^{99m}Tc (^{99m}Tc-*oxo*-core, $^{99m}Tc^{-}_{4}$) readily interacts with either electron donor groups located on the surface of iron nanoparticles, to form a chelate. In the present subsection, we summarize the recent advances on radiolabeling of iron nanomaterials with ^{99m}Tc.

Technetium-labelled uncoated iron oxide nanoparticles (IONPs) have been synthesized and characterized from the viewpoint of their behavior *in vivo* with ^{99m}Tc being utilized as an imaging agent [98]. The labeling efficiency was estimated to overcome 85% for ^{99m}Tc with IONPs, the value being highly efficient for biomedical procedures. Dynamic phase images obtained using SPECT γ-camera, illustrate the absorption of radio-labeled IONPs by brain region, occurring within the initial 15 minutes of the study. This uptake persisted for the subsequent 3 to 4 hours, the time reasonably well-suited for potential applications in anticancer drug delivery.

The introduction of novel type of dual modality imaging agents, involving the direct conjugation of radiolabeled bisphosphonates (BP) to the surface of ultrasmall superparamagnetic iron oxide nanoparticles (USPIO-NPs), was reported in [99,100]. Specifically, ^{99m}Tc-PEG-BP-USPIO-NPs were developed for combined MRI/SPECT multimodal imaging. Thorough complex *in vitro* and *in vivo* studies showed high potential of these new platforms as contrast agents for MRI angiography. Furthermore, novel USPIONPs, functionalized with BP and ^{99m}Tc were characterized by extreme stability, long blood circulation time, and require 4-fold lower dose of usage as compared to other USPIO-NPs. These advantages allowed one to recommend ^{99m}Tc-PEG-BP-USPIO-NPs as perspective assays for the multimodal medical imaging.

Dextran-coated superparamagnetic iron oxide (SPIO) nanoparticles radiolabeled with ^{99m}Tc were employed as versatile imaging agents to assess the biodistribution of NPs. This approach enabled the authors to obtain sensitive and quantitative SPECT data and high spatial resolution MRI images. The labeling efficiency and radiochemical purity of ^{99m}Tc-SPIO nanoparticles exceeded 95%, and the size of the formed radiolabeled particles corresponded to $\sim$155 nm. The synthesized ^{99m}Tc-SPIO-NPs were successfully delivered to the liver tumor either intravenously or intra-arterially. The integrated γ- and SPECT-based imaging analysis utilizing the designed nanosystems enabled perfect identification of liver tumor localization.

A novel trimodal contrast agent represented by ^{99m}Tc-labeled iron oxide/gold nanoparticles was developed by Motiei et al. [101]. The magnetic iron oxide core was used for the enhancement of MRI signals, gold and shell provided the robust CT contrast, and ^{99m}Tc was utilized to ensure SPECT imaging. The formulated hybrid nanoparticles were characterized by high labeling degree and radiochemical yield paving the way for their effective application as composite radiolabeled nanomaterial for combined multimodal SPECT/CT/MRI imaging.

A novel theranostic nanoplatform based on ^{99m}Tc-bisphosphonate-coated magnetic nanoparticles

(MNPs) has been prepared by Mirkovic and coworkers [102]. Biphosphonate coating ensured biocompatibility, colloidal stability and further successful tagging by the radionuclide. ^{99m}Tc labeling of MNPs was achieved by standard procedure using stannous chloride as the reducing agent. The labeling yield was *ca.* >95%. The characteristics of the bisphosphonate-coated magnetite NPs, including their morphology, size, structure, surface charge, and magnetic properties, were assessed using various techniques including transmission electron microscopy, X-ray powder diffraction, dynamic light scattering, laser Doppler electrophoresis, Fourier-transform infrared spectroscopy, and vibrating sample magnetometry. Importantly, nanoparticles were characterized by specific power adsorption values, signifying their capacity for generating heat, when subjected to an applied magnetic field. The synthesized ^{99m}Tc-bisphosphonate-coated MNPs preserved the stability in saline and human serum for 24 h0gts. Ex vivo biodistribution studies, supported by scintigraphic techniques, substantiated the rapid uptake of ^{99m}Tc-MNPs in the liver and spleen shortly after intravenous administration in normal Wistar rats. This behavior was attributed to the colloidal nature of the MNPs. The above advantageous characteristics of ^{99m}Tc-bisphosphonate-coated MNPs render them extremely prospective nanotheranostic agents.

5.3. Conjugation of ^{99m}Tc to silica nanomaterials

Silica nanoparticles (SNPs) exhibit significant versatility and have demonstrated broad applicability across various fields, including chemistry, biomedicine, biotechnology, agriculture, environmental remediation, and wastewater purification [104]. Their inherent characteristics, such as a mesoporous structure, high surface area, adjustable pore size, biocompatibility, modifiability, and compatibility with polymers, contribute to their expanding range of potential applications. SNPs are non-toxic and can be safely used in biomedical research. Furthermore, their ability to host molecules on both internal and external surfaces makes them excellent carriers for a wide range of compounds, whether biological or non-biological.

In pursuit of this, a novel drug delivery system based on magnetic core-mesoporous silica NPs, has been created, characterized, and assessed in vivo by Portilho *et al.* [104]. The nanoparticles were doped with dacarbazine and labeled with technetium-99m, making them suitable for use as nano-imaging agents for early and differential diagnosis of cancer using SPECT technique. *In vivo* cytotoxicity studies showed high uptake of the developed structures by liver and spleen. The analysis of NPs administration indicated that this drug delivery system effectively reached the tumor through both systemic and intratumoral routes.

The synthesis, characterization and radiolabeling with technetium-99m of mesoporous silica nanoparticles (MSNs) suitable for *in vivo* applications, was reported in [105]. A detailed physicochemical and structural analysis with the utilization of thermogravimetric analysis, Fourier transform infrared spectroscopy, zeta potential, scanning electron microscopy, low-angle X-ray diffraction and transmission electron microscopy (TEM) techniques, confirmed that the size, morphology, radiochemical yield, and main characteristics of ^{99m}Tc-MSNs were suitable for *in vivo* administration. The results of biodistribution and scintigraphic analysis showed high uptake of MSNs by liver. Notably, the particles also demonstrated significant uptake in the lungs, as indicated by a high lung-to-non-target tissues ratio. This high specificity of ^{99m}Tc-MSNs for pulmonary tissue highlights their potential for theranostic applications, particularly for drug delivery.

Silica nanoparticles labeled with technetium-99m find application in the diagnostics of inflammatory diseases as effective imaging agents. Accordingly, the potential of ^{99m}Tc-labeled mesoporous silica nanoparticles loaded with either betamethasone or dexamethasone, in the treatment and diagnostics of inflammation process, was evaluated in [106]. The formulated ^{99m}Tc-MSNs were characterized by a high degree of labeling, good pharmacokinetic profiles, and low cytotoxicity. The results of biodistribution studies in Wistar rats indicated that ^{99m}Tc-labeled mesoporous silica nanoparticles readily visualize the inflammation site with a high accumulation in the inflammatory site with substantial renal clearance.

Radiolabeling of manganese oxide-based mesoporous silica nanoparticles (Mn-MSNs) by technetium-99m to develop a novel hybrid imaging agent, was reported in [107]. In brief, a potential of newly synthesized ^{99m}Tc-Mn-MSNs as a novel dual-modal imag-

ing agent for pH-responsive MRI and SPECT studies was estimated. The ^{99m}Tc-Mn-MSNs nanoprobes exhibited increased values of T_1-weighted MRI relaxivity within the acidic tumor microenvironment and demonstrated exceptional stability and high radiolabeling efficiency. Moreover, *in vivo* MRI and SPECT imaging of tumor-bearing mice clearly revealed improved T_1-MRI and SPECT imaging of tumors, effectively combining the high spatial resolution of MRI with the outstanding sensitivity of SPECT. Furthermore, the developed nanostructures had the capacity to deliver anti-cancer drugs and release them directly at the tumor site. Collectively, these findings establish ^{99m}Tc-Mn-MSNs-PEG as an ideal nanotheranostic platform with promising applications in both biological imaging and therapy.

An innovative approach was developed to streamline the sentinel node biopsy examination through the dual-modal imaging, combining the radioactive and near-infrared fluorescent tags for visualization of deeply located sentinel nodes with anatomical precision in the surgical environment. To achieve this, the polyamidoamine (PAMAM)-coated silica nanoparticles simultaneously loaded with technetium-99m and indocyanine green have been engineered [108]. Based on the results of the animal studies, the authors concluded that the labeling of the nanoparticles both with ^{99m}Tc and indocyanine green had the synergistic effect. The surface-functionalized silica nanoparticles provided real-time visualization of sentinel lymph nodes, utilizing low concentrations of ^{99m}Tc and indocyanine green. This innovative approach has the potential to optimize the sentinel lymph node biopsy procedures and offers a novel method for targeting metastatic cells for both imaging and therapeutic purposes.

6. Labeling of organic nanomaterials with ^{99m}Tc

The labeling of organic bionanomaterials with ^{99m}Tc represents a crucial aspect in the realm of nuclear medicine, offering a powerful tool for precise and targeted imaging. Organic bionanomaterials, including polymers, lipid- and protein-based nanoparticles, lipid vesicles, and dendrimers, exhibit inherent versatility and tunable properties that make them integral components for developing advanced radiopharmaceuticals and imaging agents. The process of labeling involves the incorporation of ^{99m}Tc into organic bionanomaterials, thereby enhancing their diagnostic potential. This radiolabeling approach serves as a bridge between the unique properties of organic nanomaterials and the versatile applications of technetium-99m in nuclear medicine. The advantages of labeling organic bionanomaterials with ^{99m}Tc are manifold. First, it facilitates accurate and targeted imaging, allowing for the visualization of specific tissues or molecular targets within the body. The short half-life of ^{99m}Tc ensures a rapid decay, resulting in substantially reduced radiation exposure for patients. Moreover, the incorporation of ^{99m}Tc into organic bionanomaterials aligns with the principles of multimodal imaging. This allows for the simultaneous acquisition of various types of imaging data, providing a comprehensive and detailed understanding of the biological processes under scrutiny. In the context of theranostics, where imaging and therapeutic capabilities converge into a single platform, the radiolabeling of organic bionanomaterials with ^{99m}Tc becomes particularly impactful. It opens avenues for not only precise diagnostics, but also potential therapeutic applications, exemplifying the paradigm of personalized medicine. The utilization of technetium-99m in labeling organic bionanomaterials underscores the synergy between nanotechnology and nuclear medicine. This powerful combination contributes to the ongoing evolution of healthcare practices, offering innovative solutions for disease detection, monitoring, and treatment. As we delve into specific examples of ^{99m}Tc labeling of organic bionanomaterials, we unravel the potential of this approach in shaping the future landscape of nuclear medicine.

6.1. Lipid-based nanomaterials

Lipid nanomaterials, involving lipid nanoparticles and liposomes, are defined as organic nanomaterials that consist of lipid bilayers or monolayers enclosing an aqueous core or a solid lipid matrix, respectively. Lipid NMs have various advantages for nuclear medicine applications, such as biocompatibility, biodegradability, multifunctionality, and easy functionalization. They can be used for delivering therapeutic radioisotopes and imaging agents to targeted tissues, as well as for enhancing the contrast and resolution of nuclear imaging modalities. Labeling of liposomes and lipid nanoparticles with ^{99m}Tc is a pro-

cess that involves the attachment of radioisotope to the surface or the core of liposomes and lipid nanoparticles, either directly or indirectly, using various methods and techniques.

The conjugation of lipid NMs with ^{99m}Tc can enhance their imaging and therapeutic capabilities, as well as provide information on their biodistribution, pharmacokinetics, and biodegradation. It can also facilitate the development of theranostic liposomes and lipid nanoparticles, which can combine diagnostics and therapeutics within a single platform. The labeling of liposomes and lipid nanoparticles with ^{99m}Tc can be achieved by different methods, such as the direct labeling, indirect labeling, and pre-labeling, depending on the nature and composition of the liposomes and lipid nanoparticles and the desired stability and specificity of the radiolabel. Direct labeling involves the direct binding of ^{99m}Tc to the functional groups or the metal ions on the surface of liposomes and lipid nanoparticles, using chelating agents or covalent bonds. The indirect labeling based on the use of bifunctional chelators or linkers, which can bind to both the ^{99m}Tc and the liposomes and lipid nanoparticles, forming a stable complex. Pre-labeling relies on the synthesis of liposomes and lipid nanoparticles using ^{99m}Tc-containing precursors, resulting in the incorporation of radioisotope into the core or the shell of liposomes and lipid nanoparticles. The labeling degree of can be influenced by various factors, such as the type and activity of the ^{99m}Tc, the type and size of the liposomes and lipid nanoparticles, the labeling method and technique, the reaction conditions and parameters, the purification and quality control methods, and the storage and stability conditions.

The attachment of technetium-99m to the lipid-based NMs can be used as an effective tool for a variety of clinical applications, such as oncology, cardiology, neurology, and infection imaging, as well as radioisotope therapy. Specifically, the conjugation of liposomes with for the evaluation of colitis in Crohn's disease has been described by Brouwers et al. [109]. In this study, polyethylene glycol (PEG)-coated liposomes were labeled with ^{99m}Tc using the $[^{99m}Tc(CO)_3(H_2O)_3]^+$ precursor, which binds to the thiol groups on the liposome surface. The labeled liposomes were injected intravenously into patients with Crohn's disease and healthy volunteers, and their biodistribution and accumulation in the inflamed colon were assessed by SPECT. The results showed that the ^{99m}Tc-labeled liposomes had a long circulation time and a high uptake in the inflamed colon, indicating their potential for the diagnosis and monitoring of colitis.

In turn, the work [110] describes the labeling of lipid nanoparticles with technetium-99m for the detection of sentinel lymph nodes. Accordingly, solid lipid nanoparticles (SLNs) were labeled with ^{99m}Tc using the stannous chloride method, which reduces the ^{99m}Tc-pertechnetate to ^{99m}Tc-colloid, which then binds to the lipid matrix of the SLNs. The ^{99m}Tc-labeled SLNs were injected subcutaneously into the footpad of rats, and their migration and localization in the sentinel lymph nodes were evaluated by SPECT. The results showed that the ^{99m}Tc-labeled SLNs had a high labeling efficiency and stability, and a rapid and specific migration to the sentinel lymph nodes, indicating their potential for the detection of sentinel lymph nodes in cancer staging.

Studies by Sun *et al.* explored the direct labeling of liposomes with ^{99m}Tc using a hydrazinonicotinamide (HYNIC) derivative [111]. This method achieved a labeling efficiency of over 90% and demonstrated stability for up to 24 hours. However, the potential for nonspecific binding of the radioisotope to surface components necessitates further optimization.

The distribution of lipid NPs containing edelfosine, a powerful antitumor agent with severe adverse effects, was investigated after administration through three different routes: oral, intravenous (IV), and intraperitoneal (IP) [112]. To enable the tracking, the LNPs were labeled with 99mTc. IV administration of the radiolabeled LNPs led to fast elimination from the bloodstream and increased deposition in reticuloendothelial organs. Unfortunately, oral administration did not provide significant biodistribution data due to the formation of large radiocomplexes in the presence of gastrointestinal fluids. However, when the LNPs were administered via the IP route, they reached the systemic circulation. Remarkably, this route provided a more stable maintenance of the level of edelsofine-loaded LNPs in blood when compared to the IV route. Based on these findings, the authors propose that the IP route may be a feasible option for maintaining therapeutic drug levels in the bloodstream while avoiding excessive deposition in RES organs.

The focal point of the study [113] centered on formulating solid lipid nanoparticles loaded with cur-

cumin (C-SLNs) followed by subsequent labeling with 99mTc. The synthesis of these nanoparticles involved meticulous application of microemulsion and ultrasonication techniques, laying the groundwork for an investigation into the role of C-SLNs in liver-spleen scintigraphy. In vivo studies were conducted on New Zealand rabbits utilizing scintigraphic techniques, with a comparative analysis made against Phytate colloid, a conventional choice for liver-spleen scintigraphy. Through a detailed examination of the obtained images and biological distribution data, a significant uptake of the labeled C-SLNs in the liver and spleen was evident. These findings suggest that 99mTc-labeled C-SLNs exhibit substantial potential as an imaging agent, particularly serving as an innovative radiopharmaceutical alternative for liver and spleen imaging in colloid scintigraphy, thereby potentially revolutionizing the realm of diagnostic imaging.

The use of radiopharmaceutical based on 99mTc-labeled lipid vesicles for detection of the areas of inflammation and infection was reported in [114]. In that study, the uptake and imaging capabilities of stealth pH-sensitive liposomes labeled with technetium-99m via HMPAO complex, for detecting infection sites in mice were evaluated. These 99mTc-labeled stealth pH-sensitive liposomes were injected to mice with infections caused by Staphylococcus aureus in their right thigh muscles. Biodistribution studies and scintigraphic imaging were performed at various time intervals after the radiopharmaceutical injection. The results showed that radiolabeled liposome formulations showed significant uptake in the abscess compared to the control. The abscess was visible as early as 0.5 h after the injection of lipid vesicles, and its visibility increased over time. These findings emphasize the potential of ^{99m}Tc-labeled stealth pH-sensitive liposomes as a promising radiopharmaceutical for detecting infection sites in patients.

6.2. Protein nanomaterials

Proteins nanomaterials are emerging as another exciting class of organic bionanomaterials for ^{99m}Tc labeling. Their inherent biocompatibility and ability to interact specifically with biological targets make them ideal candidates for developing targeted diagnostic tools. However, labeling proteins with ^{99m}Tc presents unique challenges due to their complex structures and potential sensitivity to harsh labeling conditions.

Human serum albumin (HSA-NPs) nanoparticles have emerged as the most widespread in the realm of ^{99m}Tc labeling within the field of organic bionanomaterials. Their dominance can be attributed to a unique confluence of factors:

• *Biocompatibility and safety*: HSA is a naturally occurring protein found in human blood, renowned for its exceptional biocompatibility and minimal immunogenicity. This translates to minimal side effects and a high safety profile for patients undergoing diagnostic procedures with 99mTc-labeled HSA nanoparticles.

• *Efficient labeling*: HSA possesses reactive amino acid residues on its surface, offering ideal binding sites for 99mTc chelators. This allows for efficient labeling using various strategies, such as direct labeling or bioconjugation with bifunctional chelators. Studies by Straub et al. exemplify this, achieving successful labeling of HSA nanoparticles with 99mTc using a mercaptoacetyl triglycine (MAG3) chelator [115]. This efficient labeling ensures a high radiochemical yield, maximizing the amount of usable radiotracer for diagnostic imaging.

• *Versatility and targeting*: HSA nanoparticles can be readily modified to incorporate targeting moieties such as peptides or antibodies. This empowers them to home in on specific tissues or diseased cells. For instance, the development of ^{99m}Tc-labeled HSA nanoparticles conjugated with an integrin-targeting peptide has been explored [116]. These targeted nanoparticles demonstrated a significantly higher uptake in tumors compared to non-targeted counterparts, highlighting the potential for enhanced diagnostic accuracy.

• *Established niSlinical applications*: HSA nanoparticles labeled with 99mTc, often commercially available as NanoAlbumon, have become the gold standard for sentinel lymph node (SLN) scintigraphy in various cancers, particularly breast cancer and melanoma [117]. This established clinical application underscores the efficacy and safety of ^{99m}Tc-labeled HSA nanoparticles in real-world medical settings.

Various other protein-based nanomaterials have been successfully radiolabeled with technetium-99m, showcasing their versatility and potential applications in molecular imaging. In a study by Blankenberg *et al.*, annexin V, a protein known for its high specificity for apoptotic cells, was conjugated with ^{99m}Tc to enable the identification and quantification of apopto-

sis events in vivo [118]. The labeling process involved annexin V functionalization with HYNIC, leading to the formation of 99mTc-HYNIC-annexin V. This radiolabeled protein exhibited rapid elimination from the bloodstream, with a half-life of approximately 3–7 minutes, allowing for early radionuclide imaging within 60 minutes after intravenous administration in mice and rats. The rapid clearance of annexin V accurately reflected phosphatidylserine expression and apoptotic activity in the specific tissue or organ at the moment of injection.

Another study by Yang and colleagues focused on the radiolabeling process of self-assembled protein nanoparticles constructed from engineered polypeptides with His-tags for ^{99m}Tc labeling through the tricarbonyl core [119]. Liang *et al.* took a different approach by radiolabeling H-ferritin-based nanocages with 99mTc, utilizing a chelator conjugated with MAG3 through an NHS ester [120].

The application of ^{99m}Tc-labeled aprotinin in identifying cardiac amyloidosis was elegantly reviewed in [121]. The study highlighted the potential of ^{99m}Tc-labeled aprotinin as a promising radiopharmaceutical for imaging cardiopulmonary amyloidosis. The authors speculated that ^{99m}Tc-labeling of recombinant aprotinin, as opposed to the native peptide, could substantially increase the affinity of the radiopharmaceutical for amyloid fibrils, though further studies are required to validate this assumption.

Silk fibroin nanoparticles loaded with doxorubicin and radiolabeled with ^{99m}Tc were prepared to evaluate the efficacy of the drug carrier system in cellular uptake studies [122]. These nanoparticles demonstrated high in vitro stability, and cellular uptake studies on C-6 and LN-229 cell lines revealed that ^{99m}Tc-fibroin-DOX formulations exhibited greater uptake in comparison to free doxorubicin. This underscores the potential of radiolabeled silk fibroin nanoparticles as highly effective imaging agents and drug carriers for brain delivery.

6.3. Dedrimers

Dendrimers are organic nanomaterials that have a branched, tree-like structure, with a core, branches, and terminal groups. Dendrimers have various advantages for nanomedicine applications, such as biocompatibility, multifunctionality, and easy functionalization. They can be used for delivering therapeutic radioisotopes and imaging agents to targeted tissues, as well as for enhancing the contrast and resolution of nuclear imaging modalities.

Currently, two primary strategies are employed to address this challenge:

i) ***surface modification***: attaching chelator molecules directly onto the dendrimer surface offers a straightforward approach. Studies by Lee *et al.* demonstrate this method, achieving successful labeling of polyamidoamine (PAMAM) dendrimers with ^{99m}Tc using a hydrazinonicotinamide (HYNIC) derivative [123]. However, this method might suffer from potential steric hindrance due to the dense surface packing.

ii) ***core modification***: incorporating chelator moieties directly into the dendrimer core during synthesis offers another approach. This strategy ensures optimal accessibility of the chelator for ^{99m}Tc labeling. Research by Agashe *et al.* exemplifies this approach, where they synthesized the carbohydrate-coated poly(propylene imine) dendrimers for efficient 99mTc labeling [124].

The utilization of ^{99m}Tc-labeled citric acid dendrimers for targeted imaging of vascular endothelial growth factor in breast cancer was documented in a study [125]. *In vitro* cytotoxicity assessments affirmed the non-toxic nature of the resultant radiolabeled nanomaterials in normal cells, while revealing dose-dependent toxicity against cancer cells. SPECT imaging was employed to observe the in vivo accumulation of dendrimer-based nanomaterials at the tumor site, clearly indicating a substantial buildup of the radiotracer in the tumor region. These outcomes support the potential efficacy of these radiolabeled nanosystems as effective radiotracers for cancer diagnosis.

A novel radiotracer for early detection of cardiac ischemia was developed through the synthesis of composite dendrimer-peptide nanoplatforms [126]. Mutant variants of pyroglutamate helix B surface peptide were conjugated to PEGylated dendrimer-G2 and subsequently labeled with technetium-99m to detect pathological regions. The resulting conjugate exhibited high purity, labeling efficiency, and stability. Moreover, the dendrimer-based radiopharmaceutical demonstrated statistically significant affinity for binding to the surface of hypoxic cells. Biodistribution studies on the prepared ^{99m}Tc-nanoconjugate indicated elevated uptake in the cardiac ischemic region, suggesting the potential of ^{99m}Tc-

PEGylated dendrimer-G2-peptide as a valuable radiolabeled nanostructure for SPECT cardiac ischemic imaging, thereby opening new avenues in the field of diagnosis.

7. Carbon Nanomaterials Radiolabeled with ^{99m}Tc

In the field of nuclear medicine, the quest for innovative materials with superior imaging and therapeutic capabilities has led to a growing interest in the unique properties of carbon-based nanomaterials. Carbon nanomaterials (CNMs) are a diverse family of carbon allotropes with nanoscale dimensions and unique physical and chemical properties. They include fullerenes, carbon nanotubes, graphene, nanodiamonds, carbon dots, and other carbon-based nanostructures. Carbon nanomaterials have been widely explored for various applications in electronics, optoelectronics, photovoltaics, catalysis, sensing, biomedicine, just to name a few [127]. The potential of CNMs can be magnified exponentially when integrated with radiolabeling techniques. This integration empowers carbon nanomaterials to serve as carriers for radioisotope, such as ^{99m}Tc, thus expanding the horizons of molecular imaging and targeted treatments, while offering an innovative approach for tackling pressing challenges in healthcare. Labeling carbon nanomaterials with ^{99m}Tc represents a highly promising approach to harness the synergistic advantages of both constituents for applications in diagnostics and therapeutics. The utilization of ^{99m}Tc-labeled carbon nanomaterials offers a unique opportunity to gain real-time insights into the precise localization, distribution, and accumulation of these nanocarriers and their cargo within the human body, while simultaneously enabling the monitoring of their pharmacokinetics and pharmacodynamics.

One fundamental aspect of understanding and categorizing the carbon nanomaterials lies in considering their dimensionality [128]. These materials can be broadly classified into four distinct categories based on their structural dimensions:

i) ***zero-dimensional carbon nanomaterials (0D CNMs)***. In this category, carbon nanomaterials are characterized by their confinement to the nanoscale in all three dimensions. Prominent examples of 0D CNMs include fullerenes, carbon dots, and quantum dots. These materials exhibit intriguing quantum properties and find applications in nanoscale electronic devices, drug delivery, and as contrast agents in bioimaging.

ii) ***one-dimensional carbon nanomaterials (1D CNMs)***. The materials in this class extend beyond the nanoscale in one dimension while maintaining nanoscale dimensions in the other two. Carbon nanotubes (CNTs) are perhaps the most renowned representatives of 1D CNMs. These cylindrical structures exhibit remarkable mechanical strength and exceptional electrical conductivity, making them valuable in applications like nanocomposites, sensors, and nanoscale electronics.

iii) ***two-dimensional carbon nanomaterials (2D CNMs)***. 2D CNMs are characterized by their ultra-thin, nanoscale thickness. Graphene, a single layer of carbon atoms arranged in a hexagonal lattice, stands as a quintessential example in this category. Graphene's extraordinary electrical and thermal conductivity, mechanical strength, and high surface area have spurred innovations in fields such as flexible electronics, energy storage, and composite materials.

iv) ***three-dimensional carbon nanomaterials (3D CNMs)***. These materials encompass a broad range of structures with dimensions extending into the macroscopic realm, such as fibers, powders, polycrystalline structures, and multilayered configurations. Comprising a diverse mix of 0D, 1D, and 2D CNMs as building blocks, 3D CNMs offer unique advantages, including large surface areas and low densities. As a result, they hold great promise in applications such as supercapacitors, catalyst supports, and lightweight structural materials.

This section aims to provide an overview of the current state-of-the-art of the labeling of carbon nanomaterials with ^{99m}Tc, focusing on the synthesis methods, labeling mechanisms, physicochemical characterization, biological evaluation, and clinical applications of ^{99m}Tc-labeled CNMs.

7.1. Fullerenes and quantum dots

Carbon quantum dots, which are nanometer-sized carbon nanoparticles, and fullerenes, particularly the archetypal C_{60} molecule, have gained prominence due to their exceptional attributes, including tunable optical properties, biocompatibility, high stability, good conductivity, low toxicity, and versatile surface chemistry [129–131]. These characteristics make

them ideal candidates for radiolabeling and use in various nuclear medicine applications, ranging from diagnostic imaging modalities to innovative therapeutic approaches.

The potential of citrate- and polyethyleniminecapped carbon dots (C-CQs and PEI-CQDs, respectively) radiolabeled with technetium-99m, to serve as nanoagents was evaluated by Bayoumi and Emam [132]. The conjugation of the radioisotope to the CQDs was achieved by utilizing the sodium borohydride as a reducing agent. The biodistribution and tumor-targeting efficiency of the resultant radiolabeled CQDs were assessed in an Earlich ascites tumor mouse model. Both types of ^{99m}Tc-labeled CQDs exhibited high radiochemical yields and demonstrated remarkable stability. Notably, ^{99m}Tc-PEI-capped CQDs exhibited superior efficiency in targeting tumors when compared to ^{99m}Tc-citrate-capped CQDs. These findings suggest that PEI-capped CQDs hold great promise as a nanoplatform for the targeted delivery of ^{99m}Tc to tumor sites for the SPECT-based imaging.

Nanographene quantum dots (N-GQDs) were synthesized and subjected to radiolabeling with technetium-99m to facilitate the radiolabeling process of various ligands, addressing common challenges encountered in the ^{99m}Tc radiolabeling procedure, such as solvation and radioisotope binding issues [133]. Due to the exceptional water dispersion properties, N-GQDs and ligand-(N-GQD) conjugates exhibit solubility in aqueous solutions, thereby enabling the radiolabeling of water-insoluble ligands with ^{99m}Tc. The results obtained demonstrated that ^{99m}Tc could efficiently label N-GQDs, yielding a high radiochemical purity. The ^{99m}Tc-(N-GQDs) not only exemplified the radiolabeling potential of N-doped graphene quantum dots but also showcased its applicability in contexts where N-GQDs are utilized for biomedical studies. Specifically, the renal system was found to play a significant role in the clearance of ^{99m}Tc-(N-GQDs), as indicated by dosimetry studies, thus underscoring the importance of kidney as a critical organ in this context. It was proposed that N-GQDs could serve as a promising nanoplatform for enhancing solubility and radioisotope binding capabilities through the preparation of ligand-(N-GQDs) assemblies.

Ghoreishi *et al.* reviewed the effect of CQDs on the chemical properties of ^{99m}Tc [134]. Accordingly, the authors suggested that CQDs may act as reducing agents to the radioisotope and represent thereby an alternative to stannous chloride, a widely used ^{99m}Tc reducing agent. Indeed, the reducing impact of CQDs was validated through fluorescence spectroscopy, SPECT and biodistribution analysis. Furthermore, it was shown that the time of interaction, the amount of ligand and CQDs concentration affect the radiolabeling outcome.

Roeinfard *et al.* designed a novel nanoradiotracer based on labeling of selenium-functionalized PEGylated graphene quantum dots (GQDs) with ^{99m}Tc [135]. It was shown that introduction of selenium atoms during decoration of GQDs facilitates the labeling efficiency. Subsequent biodistribution studies revealed that GQDs exhibited a notably greater accumulation in the kidneys compared to other organs. This observation signifies a promising avenue for further research of ^{99m}Tc-GQDs as nanoradiopharmaceuticals, with potential applications in diagnosis, treatment, and medical imaging. The in vivo imaging aspects of this research are currently under investigation.

In their turn, Bastos and co-workers aimed their research at assessing the pharmacokinetics of GQDs, radiolabeled directly with technetium-99m, administered intravenously to Wistar rats [136]. This evaluation was conducted under two distinct temporal conditions: short-term and long-term ones. The authors postulated that the pharmacokinetic analysis conducted over an extended period offers enhanced precision and reliability. Employing a bicompartmental model, the long-term analysis discerns and accommodates each pharmacokinetic phase associated with the introduction and subsequent disposition of GQDs within the biological systems. Moreover, the data underscore that short-term analysis may yield distorted pharmacokinetic parameters, potentially leading to erroneous interpretations. In view of these findings, the significance of evaluating the pharmacokinetics of GQDs over extended timeframes, was highlighted, since it yields more meaningful insights when compared to assessments over shorter durations. The adoption of a comprehensive, long-term perspective in pharmacokinetic investigations of ^{99m}Tc-GQDs contributes to the robustness and accuracy of the data, thereby enhancing the reliability of their applications in the field of nuclear medicine and beyond.

A novel method for rapid direct ^{99m}Tc-radiolabeling of GQDs was developed to encompass the comprehensive characterization of graphene quantum dots with a focus on their *in vivo* biological performance in distinct murine models, and an evaluation of *in vitro* mutagenicity [137]. The conjugation of technetium-99m with GQDs allowed shedding light on the molecular mechanism of oxidative stress underlying the exposition to the examined quantum dots as well as on the biodistribution patterns of these nanomaterials in healthy and pathological organs.

Another type of 0D carbon-based nanomaterials is represented by fullerenes. This class of nanostructures has emerged as promising and beneficial agents in the field of nuclear medicine. They have unique features, such as spherical shape and ability to be functionalized in various ways.

The aim of work [138] was to understand the biodistribution of $C_{60}(OH)_x(O)_y$, a water-soluble C_{60} derivative, that can act as a medicinal agent or a drug carrier. The derivative was labeled with ^{99m}Tc and its distribution and metabolism in mice and rabbits were measured by using the γ-counter and SPECT methods. The results showed that the labeled compound was quickly absorbed by the tissues, and accumulated in several parts of the body, such as the skull, chest, spine, bones, liver, and spleen. However, the elimination process was slow in all tissues, except the brain. The main elimination route was through the urine and feces. The authors concluded that further studies are highly recommended to understand the biodistribution profile of radiolabeled fullerenes.

Analogous study was conducted by Qingnuan *et al.* [139]. Accordingly, C_{60} derivative $C_{60}(OH)_x$ was synthesized and labeled with ^{99m}Tc to assess the biodistribution and metabolic behavior of fullerene. The introduction of radioisotope did not change the biological characteristics of $C_{60}(OH)_x$ so the results obtained for ^{99m}Tc-$C_{60}(OH)x$ likely serve as a reliable indicator of the biological behavior of $C_{60}(OH)_x$. The examined nanostructures were found to accumulate mainly within liver, spleen, and bone, the finding being attributed to the fact that small particles are identified and sequestered by reticuloendothelial cells, thereby resulting in their retention within these specific organs. It is noteworthy that empty fullerols and similar polyhydroxylated compounds were shown previously to exhibit a pronounced affinity for cortical bone [140]. Overall, this work provides compelling evidence supporting the viability of ^{99m}Tc-$C_{60}(OH)x$ and analogous nanomaterials as prospective therapeutic agents for the treatment of conditions such as leukemia, bone cancer, and bone pain. Leveraging their favorable chemical and biological attributes, fullerene derivatives have the potential to enhance drug efficacy while mitigating toxicity. This is achievable through strategic amalgamation of fullerene with therapeutic agents and the incorporation of targeting functional groups designed to facilitate direct drug delivery to specific target tissues.

Empirical support for direct encapsulation of ^{99m}Tc into C_{60} and C_{70} during the formation of fullerenes was reported in [141]. The results of this study underscore the viability of ultra-sensitive radioactivity detection methodologies for discerning of endofullerenes. The encapsulation of radionuclides within a carbon cage holds the potential to facilitate their nonreactive transit through biological systems. By incorporating an appropriate antibody label, the radionuclide can be efficiently transported to the target site with minimal interaction between the radiolabel and the antibody.

In the present context, special attention should be given to the discussion of the so-called Technegas [142]. Technegas is a radiopharmaceutical used in nuclear medicine for pulmonary ventilation imaging. It is primarily employed in the evaluation of lung ventilation and can be instrumental in diagnosing a range of pulmonary conditions, particularly in patients with lung disorders. Technegas consists of ultrafine carbon particles, labeled with the technetium-99m [143]. When inhaled by the patient, these tiny radioactive particles disperse uniformly throughout the lungs, following the natural airflow patterns. This allows for the visualization of lung ventilation and the detection of irregularities or blockages in the airways. Technegas imaging is often used to assess lung function and to diagnose conditions such as pulmonary embolism, lung perfusion defects, and other disorders affecting lung ventilation. The advantage of using Technegas lies in its ability to provide high-resolution images of lung ventilation with minimal radiation exposure, making it a valuable tool in the diagnosis and management of lung-related medical conditions [144]. The characterization of Technegas composition and structure has undergone various interpretations and methodologies throughout

the years. In the early 1990s, Mackey *et al.* utilized a gamma camera to capture the transient, dynamic formation of Technegas during its evaporation stage from a graphite crucible [143]. Their observations revealed that Technegas was generated in a pulsed manner at temperatures near 2500 °C, with a threshold for generation at approximately 2250 °C. This process occurred concurrently with the vaporization of ^{99m}Tc atoms and the crystalline graphitic layers of the crucible. The intriguing possibility was proposed that ^{99m}Tc could integrate into fullerenes. Subsequently, Mackey *et al.* confirmed the presence of C_{60} fullerene and other fullerenes by subjecting the gas to negative-ion laser desorption Fourier transform mass spectrometry, where it was collected as a film on a stainless-steel substrate. It was postulated by Mackey *et al.* that the fullerene structures formed during the Technegas generation process might undergo transformation into metallofullerenes, wherein a technetium atom attaches to the fullerene either in an endohedral or exohedral form [143].

However, the detection and confirmation of fullerenes in Technegas have not been consistent across different studies, and the debate continues. Some researchers have raised questions about whether the primary particles in Technegas contain fullerenes or whether fullerenes are present but undetectable using conventional techniques [145, 146]. While there have been suggestions and studies proposing the presence of fullerenes in Technegas, the definitive confirmation remains a topic of ongoing research and scientific inquiry. Further studies and advancements in analytical techniques may provide more conclusive evidence regarding the presence or absence of fullerenes in Technegas.

7.2. Graphene

Graphene is a one-atom-thick layer of carbon atoms arranged in a hexagonal lattice. Graphene has many remarkable properties, such as high stability, good conductivity, low toxicity, environmental friendliness, and tunable optical properties [147, 148]. Its exceptional electrical, thermal, and mechanical properties, along with its versatile surface chemistry, enabled graphene exploration for applications in various fields such as optoelectronics, photovoltaics, sensing, biomedicine, and others. Labeling of graphene with radioactive isotopes, such as technetium-99m, is a promising strategy to combine the advantages of both graphene and radiotracers for diagnostic and therapeutic applications, and to form novel radiotracers for nuclear medicine multimodal imaging [149].

The antibacterial activity of graphene oxide (GO) sheets against Gram-positive bacteria, such as *Staphylococcus aureus*, was evaluated [149] through the radiolabeling of GO with technetium-99m. To assess the *in vivo* performance of ^{99m}Tc-labeled GO, the biodistribution studies were conducted in Swiss Albino rats with experimentally induced infections in the left lateral thigh, employing *S. aureus* as the pathogen. The biodistribution study showed that the maximum accumulation of ^{99m}Tc-GO at the infection sites occurred at 60 min post-injection. The revealed accumulation of radiolabeled graphene oxide within experimentally induced infection foci in rats serves as a substantive validation of the efficacy of examined radiopharmaceutical in targeting the infectious lesions.

Jiang *et al.* reported on the synthesis and radiolabeling of GO nanosheets with ^{99m}Tc to develop a versatile SPECT imaging agent [150]. GO nanosheets were prepared by the modified Hummers' method, and then were functionalized with azide groups by a two-step reaction. Afterwards, GO nanosheets were functionalized with DOTA and alkynyl groups to enable the radiolabeling with ^{99m}Tc. The synthesized DOTA-conjugated GOs, with lateral dimensions ranging from 500 to 600 nm, were characterized using the atomic force microscopy and Fourier-transform infrared spectroscopy. Remarkably, the labeling efficiency and radiochemical purity of GO-DOTA with ^{99m}Tc exceeded 90% and 96%, respectively. The successful synthesis of these graphene oxide derivatives, and subsequent labeling with ^{99m}Tc for SPECT imaging, underscores their potential as highly efficient platforms for future molecular imaging research endeavors.

To assess the impact of surface functionalization on the theranostic potential of graphene, Sasidharan and coworkers synthesized few-layer graphene (FLG) and its carboxylated (FLG-COOH) and PEGylated (FLG-PEG) derivatives. To track dynamically the kinetics of *in vivo* accumulation, biodistribution profile and systemic clearance in Swiss albino mice, these nanomatrices were covalently tagged with ^{99m}Tc [151]. Intriguingly, the examination of organ biodistribution properties, conducted through radiographic imaging and histological investigations,

unveiled the enduring presence of both FLG and FLG-COOH in the lung, liver, spleen, and kidney with the manifestation of severe pathological alterations, encompassing acute-to-chronic inflammation, pulmonary edema, granuloma formation, interstitial nephritis, and structural impairment in the liver and spleen. In contrast, among animals administered with FLG-PEG, critical assessments of vital organs revealed an absence of noteworthy abnormalities. Thus, ^{99m}Tc-FLG-PEG may be recommended as safe nanoradiotracer for different imaging modalities.

To harness the potential of graphene oxide nanoribbons (GONRs) in synergy with chemo-photothermal therapy, phospholipid-polyethylene glycol (PL-PEG)-functionalized GONRs were tagged with technetium-99m [152]. The results unveiled a distinctive biodistribution profile for the ^{99m}Tc-labeled PL-PEG-GONRs in murine animal model, characterized by prompt accumulation within the liver, followed by efficient excretion. Notably, it was established that the renal route was the primary mode of excretion, with urinary elimination of PL-PEG-GONRs. Moreover, ^{99m}Tc-PL-PEG-GONRs loaded with doxorubicin exhibited half maximal inhibitory concentration values for chemo-photothermal therapy against U87 glioma cells that were 6.7-fold lower than those in conventional chemotherapy. This underscores the potential of ^{99m}Tc-PL-PEG-GONRs as nanocarriers for drug delivery with real time detection and visualization, offering an efficacious cancer therapy approach that not only enhances treatment effectiveness but also minimizes the risk of adverse side effects associated with the nanocarrier within the biological system.

The objective of the study reported by Yurt *et al.* was to radiolabel ampicillin-loaded graphene oxide nanoflakes (AMP-GO) with technetium-99m and assess their in vitro binding affinity to *Staphylococcus aureus* and *Escherichia coli* bacteria [153]. The characterization of AMP-GO was accomplished using Fourier-transform infrared spectroscopy (FTIR) and scanning electron microscopy (SEM). Both AMP and AMP-GO were subsequently radiolabeled with ^{99m}Tc using stannous chloride as a reducing agent, resulting in a labeling efficiency of ∼98%. Notably, ^{99m}Tc-AMP-GO exhibited significantly higher binding affinities to both *S. aureus* and *E. coli* when compared to ^{99m}Tc-AMP. This suggests that ^{99m}Tc-AMP-GO holds promise as a potential agent for infection nuclear imaging.

7.3. Carbon nanotubes

Carbon nanotubes (CNTs) are cylindrical assemblies that consist of rolled-up sheets of single-layer carbon atoms (graphene). They have diameters in the nanometer range and lengths up to millimeters [154]. They possess unique properties such as high aspect ratio, mechanical strength, electrical and thermal conductivity, chemical stability, and a tip-surface area near the theoretical limit. The distinctive physical properties of carbon nanotubes render them highly appealing within the domain of biomedical imaging. In this regard, a special attention is given to conjugation of CNTs with radionuclides to increase the versatility of CNT-based nanoprobes [155].

Accordingly, Datit *et al.* developed the therapeutic conjugate based on multiwalled carbon nanotubes (MWCNTs), functionalized with hyaluronic acid, and doped with doxorubicin. To ensure the analysis of intracellular trafficking and biodistribution of the nanocomposite, MWCNTs were concomitantly labeled with both fluorescent dye and ^{99m}Tc [156]. The conjugation with ^{99m}Tc involved the standard protocol of radiolabeling using the stannous chloride as a reducing agent. The labeling efficiency was reported to exceed 98%. The results obtained revealed the prolonged toxicity of the labelled MWCNTs, suggesting that the developed nanocarrier platform has the potential to broaden the scope of therapeutic options for various anticancer drugs and may be recommended for potential clinical applications.

The study reported by Wang *et al.*, focuses on the development of radiolabeled, iron oxide-decorated multiwalled carbon nanotubes designed to function as dual contrast agents for magnetic resonance imaging and single photon emission computed tomography [157]. The composites, incorporating varied quantities of iron oxide, were effectively radiolabeled with technetium-99m using a functionalized bisphosphonate, enabling SPECT/CT imaging and γ-scintigraphy to quantitatively analyze the distribution within mice. Histological examinations revealed no abnormalities, with Perls stain confirming the presence of superparamagnetic iron oxide nanoparticles (SPIONs) and Neutral Red stain identifying the MWCNTs. Transmission electron microscopy images of liver and spleen tissues showcase the colocalization of SPION and MWCNTs within the same intracellular vesicles, indicating the stability of the

composite post intravenous injection. The findings underscore the potential of the SPION-MWCNT hybrids as dual MRI and SPECT contrast agents for *in vivo* applications, exhibiting promising capabilities in biomedical imaging and targeted drug delivery systems.

To assess the toxicity and biodistribution pattern in tumor-bearing mice models, de Alcantara Lemos et al. radiolabeled PEGylated MWCNTs with ^{99m}Tc [158]. The results of the study indicate that the developed system exhibits an extended duration of blood circulation and demonstrates significant uptake rates in tumor tissues. Evaluation of toxicological data obtained from experimentation on healthy animal subjects revealed that PEGylated multiwalled carbon nanotubes did not provoke a notable toxic profile. Taking into consideration all the findings obtained in this study, the authors concluded that PEG-coated MWCNTs hold promise as a potential candidate for future applications in oncology.

To leverage the cytotoxic potential of mesoporous carbon nanotubes (mCNTs) Du and coworkers investigated the toxicity and biodistribution of both pristine and surface-modified mCNTs [159]. Tracing with ^{99m}Tc indicated that the cellular uptake of pristine mCNTs followed a concentration-dependent and energy-reliant process, engaging macropinocytotic and clathrin-dependent pathways. The principal accumulation sites were identified as the lung, liver, and spleen. Upon surface modification, there was a conspicuous reduction in generation of reactive oxygen species, MDA accumulation, and superoxide dismutase depletion compared to pristine mCNTs. The mechanisms of internalization and organ distribution remained mostly unchanged following the modification. Collectively, this report demonstrated that ^{99m}Tc-labeled mCNTs serve as effective tracers for mapping nanotube distribution within living organisms.

The work by Wei *et al.* [160] employs technetium-99 as the radiolabeling isotope to investigate the biodistribution of oxidized multi-walled carbon nanotubes (oMWCNTs) and nanodiamonds (NDs) upon intravenous administration in mice. The histological effects of non-radiolabeled oMWCNTs or NDs were evaluated in comparison to combined exposure groups. The ^{99m}Tc-labeled nanomaterials exhibited notable *in vivo* stability and rapid clearance from the bloodstream. Following a singular injection of oMWCNTs, the most significant accumulation was observed in the lungs, with relatively lower uptake in the liver and spleen. Conversely, standalone administration of NDs resulted in substantial distribution within the liver, spleen, and lungs immediately post-injection. Co-administration of oMWCNTs and NDs significantly altered the *in vivo* distribution pattern of NDs, with varying doses of oMWCNTs affecting hepatic and splenic accumulation of NDs and elevating lung retention. In contrast, NDs had minimal impact on the distribution of oMWCNTs in mice. This study uncovered the molecular mechanisms underlying the co-administration of different nanomaterials.

The radiolabeling of carboxylated and bisphosphonate single-walled carbon nanotubes (SWCNTs) with ^{99m}Tc were described by Fernandes *et al.* [161]. Both types of nanotubes exhibited significant stability, ensuring their potential for continued utilization in subsequent in vivo experiments. Blood clearance studies revealed that bisphosphonate SWCNTs show a half-life ∼50% longer than ^{99m}Tc-labeled carboxylated SWCNTs proposing the functionalization with bisphosphonate as a promising approach to extend blood circulation duration and thereby to enhance tumor accumulation. Further *in vivo* experiments validated the selective accumulation of bisphosphonate SWCNTs within the tumor site, thus demonstrating their biocompatibility.

8. Conclusions and Future Perspectives

The successful radiolabeling of nanomaterials with technetium-99m opened up the exciting possibilities for advancing personalized medicine through targeted imaging and therapy. The versatility and sensitivity of ^{99m}Tc radiolabeling enable tailored approaches for different disease diagnostics and treatments. This technology holds substantial promise for addressing unmet clinical needs and advancing precision medicine. Radiolabeling with ^{99m}Tc demonstrates robustness in providing real-time data on biodistribution, allowing for a better understanding of how nanomaterials interact within the organism. The studies reviewed in the present work revealed consistent and reliable labeling methods that present an opportunity to advance personalized medicine through tailored diagnostic imaging and targeted therapy.

The ongoing research and advancement of technetium-99m radiolabeling for nanomaterials marks a pioneering field in biomedical research. The prospects

and potential avenues for development comprise the following key areas:

• enhanced targeting strategies: innovations in targeting mechanisms can escalate the precision and specificity of nanomaterial delivery to designated sites. The modification of surface characteristics of nanomaterials to amplify their association with formally identified cell types or tissues has immense potential for development.

• Stability and longevity: further investigation is essential to enhance the stability and endurance of radiolabeled nanomaterials whilst exposed to physiological environment. This will ensure elongated circulating times and improve efficiency in diagnoses and therapy.

• Clinical translation: progressing towards clinical deployments calls for a comprehensive grasp of the safety profiles, toxicity, and regulatory requirements of ^{99m}Tc-labeled nanomaterials. Such investigations will help in creating the innovative diagnostic and therapeutic tools with sufficient practicality.

• Multimodal imaging: exploring the potential of combining technetium-99m radiolabeling with other imaging modalities could provide a more comprehensive view of biodistribution and enhance diagnostic accuracy. Integrating multiple imaging techniques may offer a more holistic understanding of disease progression and treatment response.

• Nanomaterial diversity: investigating a wider spectrum of nanomaterials and their radiolabeling potential could expand the applications of technetium-99m in diverse biomedical fields, ranging from cardiovascular diseases to neurological disorders.

The advancement and optimization of technetium-99m radiolabeling techniques for nanomaterials hold promise for revolutionizing the landscape of personalized medicine. Continued research and development in this area are vital for realizing the full potential of technetium-99m-labeled nanomaterials in clinical practice.

APPENDIX. Abbreviations

^{99m}Tc	technetium-99m
AgNPs	silver nanoparticles
AMP-GO	ampicillin-loaded graphene oxide nanoflakes
AuNMs	gold nanomaterials
AuNPs	gold nanoparticles
BP	bisphosphonates
C-CQDs	citrate-capped carbon dots
CNFs	carbon nanofibers
CNMs	carbon nanomaterials
CNTs	carbon nanotubes
CQDs	carbon quantum dots
CT	computer tomography
DOX	doxorubicin
FLG	few-layer graphene
FLG-COOH	carboxylated few-layer graphene
FLG-PEG	PEGylated few-layer graphene
FTIR	Fourier transform infrared
GO	graphene oxide
GONRs	graphene oxide nanoribbons
GQDs	graphene quantum dots
HSA	human serum albumin
HYNIC	2-hydrazinonicotinic acid
IONPs	iron oxide nanoparticles
IP	intraperitoneal
IV	intravenous
MAG3	mercaptoacetyl triglycine
mCNTs	mesoporous carbon nanotubes
MNPs	magnetic nanoparticles
MR	magnetic resonance
MRI	magnetic resonance imaging
MSNs	mesoporous silica nanoparticles
MWCNTs	multiwalled carbon nanotubes
nD CNMs	n-dimensional carbon nanomaterials
NDs	nanodiamonds
N-GQDs	nanographene quantum dots
NMs	nanomaterials
oMWCNTs	oxidized multi-walled carbon nanotubes
PAMAM	polyamidoamine
PDI	polydispersity index
PEG	polyethylene glycol
PEI-CQDs	polyethylenimine-capped carbon dots
PET	positron emission tomography
PL-PEG	phospholipid-polyethylene glycol
SEM	scanning electron microscopy
SLN	sentinel lymph node
SLNs	solid lipid nanoparticles
SNPs	silica nanoparticles
SPECT	single photon emission computed tomography
SPIO	superparamagnetic iron oxide
SPIONs	superparamagnetic iron oxide nanoparticles
SWCNTs	single-walled carbon nanotubes
TEM	transmission electron microscopy
USPIO-NPs	ultrasmall superparamagnetic iron oxide nanoparticles

1. M. Djekidel. The changing landscape of nuclear medicine and a new era: the "NEW (Nu) CLEAR Medicine": A framework for the future. Front. Nucl. Med. **3**, 1213714 (2023).
2. H. Duan, A. Iagaru, C. Aparici. Radiotheranostics – precision medicine in nuclear medicine and molecular imaging. *Nanotheranostics* **6**, 103 (2022).

3. J. Czernin, I. Sonni, A. Razmaria, J. Calais. The future of nuclear medicine as an independent specialty. *J. Nucl. Med.* **60**, 3S (2019).
4. A. Zwanenburg. Radiomics in nuclear medicine: robustness, reproducibility, standardization, and how to avoid data analysis traps and replication crisis. *Eur. J. Nucl. Med. Mol. Imaging.* **46**, 2638 (2019).
5. K. Vermeulen, M. Vandamme, G. Bormans, F. Cleeren. Design and challenges of radiopharmaceuticals. *Seminars Nucl. Med.* **49**, 339 (2019).
6. Z. Morris, A. Wang, S. Knox. The radiobiology of radiopharmaceuticals. *Seminars Rad. Oncol.* **31**, 20 (2021).
7. I. Roy, S. Krishnan, A. Kabashin, I. Zavestovskaya, P. Prasad. Transforming nuclear medicine with nanoradiopharmaceuticals. *ACS Nano.* **16**, 5036 (2000).
8. J. Ge, Q. Zhang, J. Zeng, Z. Gu, M. Gao. Radiolabeling nanomaterials for multimodality imaging: new insights into nuclear medicine and cancer diagnosis. *Biomaterials.* **228**, 119553 (2020).
9. A. Singh, M. Amiji. Application of nanotechnology in medical diagnosis and imaging. *Curr. Opin. Biotechnol.* **74**, 241 (2022).
10. J. Pellico, P. Gawne, R. de Rosales. Radiolabelling of nanomaterials for medical imaging and therapy. *Chem. Soc. Rev.* **50**, 3355 (2021).
11. L. Farzin, S. Sheibani, M. Moassesi, M. Shamsipur. An overview of nanoscale radionuclides and radiolabeled nanomaterials commonly used for nuclear molecular imaging and therapeutic functions. *J. Biomed. Mater. Res. Part A* **107**, 251 (2019).
12. C. Ferreira, D. Ni, Z. Rosenkrans, W. Cai. Radionuclide-activated nanomaterials and their biomedical applications. *Angew. Chem.* **58**, 13232 (2019).
13. A. Ruggiero, C. Villa, J. Holland, S. Sprinkle, C. May, J. Lewis, D. Scheinberg, M. McDevitt. Imaging and treating tumor vasculature with targeted radiolabeled carbon nanotubes. *Int. J. Nanomedicine.* **5**, 783 (2010).
14. N. Tang, Y. Wei, Q. Yang, Y. Yang, M. Sailor, H.-B. Pang. Rapid chelator-free radiolabeling of quantum dots for in vivo imaging. *Nanoscale.* **11**, 22248 (2019).
15. F. Ai, C. Ferreira, F. Chen, W. Cai. Engineering of radiolabeled iron oxide nanoparticles for dual-modality imaging. Wiley Interdiscip. *Rev. Nanomed. Nanobiotechnol.* **8**, 619 (2016).
16. N. Daems, C. Michiels, S. Lucas, S. Baatout, A. Aerts. Gold nanoparticles meet medical radionuclides. *Nucl. Med. Biol.* **100**, 61 (2021).
17. J. Xie, K. Chen, J. Huang, S. Lee, J. Wang, J. Gao, X. Li, X. Chen. PET/NIRF/MRI triple functional iron oxide nanoparticles. *Biomaterials. 31*, 3016 (2010).
18. A. Amraee, Z. Alamzadeh, R. Irajirad, A. Sarikhani, H. Ghaznavi, H. Harvani, S. Mahdavi, S. Shirvalilou, S. Khoei. Theranostic RGD@Fe3O4-Au/Gd NPs for the targeted radiotherapy and MR imaging of breast cancer. *Cancer Nano* **14**, 61 (2023).
19. D. Psimadas, P. Bouziotis, P. Georgoulias, V. Valotassiou, T. Tsotakos, G. Loudos. Radiolabeling approaches of nanoparticles with ^{99m}Tc. *Contrast Media Mol. Imaging.* **8**, 333 (2013).
20. S. Mushtaq, A. Bibi, J. Park, J. Jeon. Recent progress in technetium-99m-labeled nanoparticles for molecular imaging and cancer therapy. *Nanomaterials (Basel).* **11**, 3022 (2021).
21. R. Santos-Oliveira, L. Antunes. Radiopharmaceutical research and production in Brazil: A 30-year history of participation in the nuclear medicine scenario. *J. Nucl. Med. Technol.* **39**, 237 (2011).
22. M. Billinghurst, S. Rempel, B. Westendorf. Radiation decomposition of technetium-99m radiopharmaceuticals. *Phys. Rad. Biol.* **20**, 138 (1979).
23. K. Bannister, S. Penglis, J. Bellen, R. Baker, B. Chatterton. Kit preparation of technetium-99m-mercaptoacetyltriglycine: Analysis, biodistribution and comparison with technetium-99m-DTPA in patients with impaired renal function. *J. Nucl. Med.* **31**, 1568 (1990).
24. C. Perrier, E. Segrè. Some chemical properties of element 43. *J. Chem. Phys.* **5**, 712 (1937).
25. E. Segrè, G. Seaborg. Nuclear isomerism in element 43. *Phys. Rev.* **55**, 808 (1939).
26. J. Weaver, C. Soderquist, N. Washton, A. Lipton, P. Gassman, W. Lukens, A. Kruger, N. Wall, J. McCloy. Chemical trends in solid alkali pertechnetates. *Inorg. Chem.* **56**, 2533 (2017).
27. A. Davison, A. Jones. The chemistry of technetium (V). *Int. J. Appl. Radiat. Isot.* **33**, 875 (1982).
28. S. Liu, D. Edwards, J. Barrett. ^{99m}Tc labeling of highly potent small peptides. *Bioconjug. Chem.* **8**, 621 (1997).
29. S. Rathmann, Z. Ahmad, S. Slikboer, H. Bilton, D. Snider, J. Valliant. The radiopharmaceutical chemistry of Technetium-99m. In: *Radiopharmaceutical Chemistry.* Edited by J. Lewis, A. Windhorst, B. Zeglis (Springer, 2019), pp. 311.
30. R. Alberto. The particular role of radiopharmacy within bioorganometallic chemistry. *J. Organomet. Chem.* **192**, 1179 (2007).
31. A. Boschi, L. Uccelli, P. Martini. A picture of modern Tc-99m radiopharmaceuticals: production, chemistry, and applications in molecular imaging. *Appl. Sci.* **9**, 2526 (2019).
32. G. Mariani, L. Bruselli, T. Kuwert, E. Kim, A. Flotats, O. Israel, M. Dondi, N. Watanabe. A review on the clinical uses of SPECT/CT. *Eur. J. Nucl. Med. Mol. Imaging.* **37**, 1959 (2010).
33. O. Israel, O. Pellet, L. Biassoni, D. De Palma, E. Estrada-Lobato, G. Gnanasegaran, T. Kuwert, C. la Fougère, G. Mariani, S. Massalha, D. Paez, F. Giammarile. Two decades of SPECT/CT – the coming of age of a technology: An updated review of literature evidence. *Eur. J. Nucl. Med. Mol. Imaging.* **46**, 1990 (2019).
34. T. Saleh. Technetium-99m radiopharmaceuticals. In: *Basic Sciences of Nuclear Medicine.* Edited by M. Khalil (Springer, 2010).

35. B. Mandalapu, M. Amato, H. Stratmann. Technetium Tc 99m sestamibi myocardial perfusion imaging: current role for evaluation of prognosis. *Chest.* **115**, 1684 (1999).
36. H. Ziessman, J. O'Malley, J. Thrall. *Nuclear Medicine: The Requisites.* 4^{th} ed. (Elsevier Health Sciences, 2013) [ISBN: 978-0-323-08299-0].
37. T. Hussain, Q. Nguyen. Molecular imaging for cancer diagnosis and surgery. *Adv. Drug Deliv. Rev.* **66**, 90 (2014).
38. W. Pardridge. Blood-brain barrier delivery. *Drug Discov. Today.* **12**, 54 (2007).
39. N. Joudeh, D. Linke. Nanoparticle classification, physicochemical properties, characterization, and applications: A comprehensive review for biologists. *J. Nanobiotechnol.* **20**, 262 (2022).
40. S. Abbina, L. Takeuchi, P. Anilkumar, K. Yu, J. Rogalski, R. Shenoi, I. Constantinescu, J. Kizhakkedathu. Blood circulation of soft nanomaterials is governed by dynamic remodeling of protein opsonins at nano-biointerface. *Nat. Commun.* **11**, 3048 (2020).
41. B. Mekuye, B. Abera. Nanomaterials: An overview of synthesis, classification, characterization, and applications. *Nano Select.* **4**, 486 (2023).
42. B. Alshammari, M. Lashinb, M. Mahmood, F. Al-Mubaddelde, N. Ilyasf, N. Rahman, M. Sohail, A. Khan, S. Abdullaev, R. Khan. Organic and inorganic nanomaterials: Fabrication, properties and applications. *RCS Adv.* **13**, 13735 (2023).
43. K. Khalid, X. Tan, H. Zaid, Y. Tao, C. Chew, D. Chu, M. Lam, Y. Ho, J. Lim, L. Wei. Advanced in developmental organic and inorganic nanomaterial: A review. *Bioengineered.* **11**, 328 (2020).
44. D. Lombardo, P. Calandra, L. Pasqua, S. Magazù. Self-assembly of organic nanomaterials and biomaterials: The bottom-up approach for functional nanostructures formation and advanced applications. *Materials* **13**, 1048 (2020).
45. G. Speranza. Carbon nanomaterials: Synthesis, functionalization and sensing applications. *Nanomaterials.* **11**, 967 (2021).
46. D. Holmannova, P. Borsky, T. Svadlakova, L. Borska, Z. Fiala. Carbon nanoparticles and their biomedical applications. *Appl. Sci.* **12**, 7865 (2022).
47. L. Porto, D. Silva, A. de Oliveira, A. Pereira, K. Borges. Carbon nanomaterials: Synthesis and applications to development of electrochemical sensors in determination of drugs and compounds of clinical interest. *Rev. Anal. Chem.* **38**, 20190017 (2019).
48. R. Onyancha, K. Ukhurebor, U. Aigbe, O. Osibote, H. Kusuma, H. Darmokoesoemo. A methodical review on carbon-based nanomaterials in energy-related applications. *Ads. Sci. Technol.* **2022**, 4438286 (2022).
49. P. Martini, M. Pasquali, A. Boschi, L. Uccelli, M. Giganti, A. Duatti. Technetium complexes and radiopharmaceuticals with scorpionate ligands. *Molecules.* **23**, 2039 (2018).
50. U. Abram, R. Alberto. Technetium and rhenium – coordination chemistry and nuclear medical applications. *J. Braz. Chem. Soc.* **17**, 1486 (2006).
51. K. Thipyapong, T. Uehara, Y. Tooyama, H. Braband, R. Alberto, Y. Arano. Insight into technetium amidoxime complex: Oxo technetium (V) complex of N-substituted benzamidoxime as new basic structure for molecular imaging. *Inorg. Chem.* **50**, 992 (2011).
52. C. Bolzati, A. Dolmella. Nitrido technetium-99m core in radiopharmaceutical applications: Four decades of research. *Inorganics* **8**, 3 (2020).
53. M. Pasquali, E. Janevik-Ivanovska, A. Duatti. Technetium nitrido-peroxo complexes: an unexplored class of coordination compounds. *Inorganics* **7**, 142 (2019).
54. J. Baldas. Chemistry of technitium nitrido complexes. *Pure Appl. Chem.* **62**, 1079-80 (1990).
55. C. Decristoforo, S. Mather. 99m-Technetium-labelled peptide-HYNIC conjugates: Effects of lipophilicity and stability on biodistribution. *Nucl. Med. Biol.* **26**, 389 (1999).
56. M. Surfraz, R. King, S. Mather, S. Biagini, P. Blower. Technetium-binding in labelled HYNIC-peptide conjugates: role of coordinating amino acids. *J. Inorg. Biochem.* **103**, 971 (2009).
57. L. Meszaros, A. Dose, S. Biagini, P. Blower. Hydrazinonicotinic acid (HYNIC) – coordination chemistry and applications in radiopharmaceutical chemistry. *Inorg. Chim. Acta.* **363**, 1059 (2010).
58. B. Li, S. Hildebrandt, A. Hagenbach, U. Abram. Tricarbonylrhenium(I) and -technetium(I) complexes with tris(1,2,3-triazolyl)phosphine oxides. *Z. Anorg. Allg. Chem.* **647**, 1070 (2021).
59. S. Mather, D. Ellison. Reduction-mediated technetium-99m labeling of monoclonal antibodies. *J. Nucl. Med.* **31**, 692 (1990).
60. E. Joiris, B. Bastin, J. Thornback. A new method for labelling of monoclonal antibodies and their fragments with technetium-99m. *Int. J. Rad. Appl. Instrum. B* **18**, 353 (1991).
61. R. Mease, C. Lambert. Newer methods of labeling diagnostic agents with Tc-99m. *Seminars Nucl. Med.* **31**, 278 (2001).
62. A. Bao, B. Goins, R. Klipper, G. Negrete, W. Phillips. Direct ^{99m}Tc labeling of pegylated liposomal doxorubicin (Doxil) for pharmacokinetic and non-invasive imaging studies. *J. Pharmacol. Exp. Ther.* **308**, 419 (2004).
63. M. Pijeira, H. Viltres, J. Kozempel, M. Sakmár, M. Vlk, D. İlem-Özdemir, M. Ekinci, S. Srinivasan, A. Rajabzadeh, E. Ricci-Junior, L. Alencar, M. Qahtani, R. Santos-Oliveira. Radiolabeled nanomaterials for biomedical applications: Radiopharmacy in the era of nanotechnology. *EJNMMI Radiopharm. Chem.* **7**, 8 (2022).
64. M. Mariscal, J. Olmos-Asar, C. Gutierrez-Wing, A. Mayoral, M. Yacaman. On the atomic structure of thiol-protected gold nanoparticles: a combined experimental

and theoretical study. *Phys. Chem. Chem. Phys.* **12**, 11785 (2010).
65. D. Bonvin, J. Bastiaansen, M. Stuber, H. Hofmann, M. Ebersold. Chelating agents as coating molecules for iron oxide nanoparticles. *RSC Adv.* **7**, 55598 (2017).
66. H. Yamaguchi, M. Tsuchimochi, K. Hayama, T. Kawase, N. Tsubokawa. Dual-labeled near-infrared/(99m)Tc imagingp using PAMAM-coated silica nanoparticles for the Imaging of HER2-expressing cancer cells. *Int. J. Mol. Sci.* **17**, 1086 (2016).
67. E. Vitorge, S. Szenknect, J. Martins, V. Barthès, A. Auger, O. Renard, J. Gaudet. Comparison of three labeled silica nanoparticles used as tracers in transport experiments in porous media. Part I: Syntheses and characterizations. *Environm. Poll.* **184**, 605 (2014).
68. P. Biehl, F. Schacher. Surface functionalization of magnetic nanoparticles using a thiol-based grafting-through approach. *Surfaces.* **3**, 116 (2020).
69. Z. Salehi, H. Ghahfarokhi, A. Kodadadi, R. Rahimnia. Thiol and urea functionalized magnetic nanoparticles with highly enhanced loading capacity and thermal stability for lipase in transesterification. *J. Industr. Engineer. Chem.* **35**, 224 (2016).
70. L. Aranda-Lara, K. Isaac-Olivé, B. Ocampo-García, G. Ferro-Flores, C. González-Romero, A. Mercado-López, R. García-Marín, C. Santos-Cuevas, J. Estrada, E. Morales-Avila. Engineered rHDL nanoparticles as a suitable platform for theranostic applications. *Molecules.* **27**, 7046 (2022).
71. L. Aranda-Lara, E. Morales-Avila, M. Luna-Gutiérrez, E. Olivé-Alvarez, K. Isaac-Olivé. Radiolabeled liposomes and lipoproteins as lipidic nanoparticles for imaging and therapy. *Chem. Phys. Lipids.* **230**, 104934 (2020).
72. P. Laverman, E. Dams, W. Oyen, G. Storm, E. Koenders, R. Prevost, J. van der Meer, F. Corstens, O. Boerman. A novel method to label liposomes with ^{99m}Tc by the hydrazino nicotinyl derivative. *J. Nucl. Med.* **40**, 192 (1999).
73. P. Laverman, L. Bloois, O. Boerman, W. Oyen, F. Corstens, G. Storm. Lyophilization of TC-99m-Hynic labeled PEG-liposomes. *J. Liposome Res.* **10**, 117 (2000).
74. V. Pandey, T. Haider, A. Chandak, A. Chakraborty, S. Banerjee, V. Soni. Technetium labeled doxorubicin loaded silk fibroin nanoparticles: optimization, characterization and in vitro evaluation. *J. Drug Deliv. Sci. Technol.* **56**, 101539 (2020).
75. R. Sharma. Labeling efficiency and biodistribution of Technetium-99m labeled nanoparticles: interference by colloidal tin oxide particles. *Int. J. Pharm.* **289**, 189 (2005).
76. S. Wu, E. Helal-Neto, A. dos Santos Matos, A. Jafari, J. Kozempel, Y. de Albuquerque Silva, C. Serrano-Larrea, S. Junior, E. Ricci-Junior, F. Alexis, R. Santos-Oliveira. Radioactive polymeric nanoparticles for biomedical application. *Drug Delivery* **27**, 1544 (2020).
77. V. Trubetskoy. Polymeric micelles as carriers of diagnostic agents. *Adv. Drug Deliv. Rev.* **37**, 81 (1999).
78. M. Roeinfard, M. Zahedifar, M. Darroudi, K. Sadri, A. Zak. Preparation of technetium labeled-graphene quantum dots and investigation of their bio distribution. *J. Cluster Sci.* **33**, 965 (2022).
79. N. Bayoumi, A. Emam. ^{99m}Tc radiolabeling of polyethylenimine capped carbon dots for tumor targeting: synthesis, characterization and biodistribution. *Int. J. Radiat. Biol.* **97**, 977 (2021).
80. L. Kovacs, M. Tassano, M. Cabrera, M. Fernández, W. Porcal, R. Anjos, P. Cabral. Labeling polyamidoamine (PAMAM) dendrimers with technetium-99m via hydrazinonicotinamide (HYNIC). *Curr. Radiopharm.* **7**, 115 (2014).
81. S. Ghoreishi, A. Khalaj, O. Sabzevari, L. Badrzadeh, P. Mohammadzadeh, S. Mousavi Motlagh, A. Bitarafan-Rajabi, M. Shafiee Ardestani. Technetium-99m chelator-free radiolabeling of specific glutamine tumor imaging nanoprobe: In vitro and in vivo evaluations. *Int. J. Nanomedicine* **13**, 4671 (2018).
82. M. Podolska, A. Barras, C. Alexiou, B. Frey, U. Gaipl, R. Boukherroub, S. Szunerits, C. Janko, L. Muñoz. Graphene oxide nanosheets for localized hyperthermia – physicochemical characterization, biocompatibility, and induction of tumor cell death. *Cells* **9**, 776 (2020).
83. S. Challan, A. Massoud. Radiolabeling of graphene oxide by Technetium-99m for infection imaging in rats. *J. Radioanal. Nucl. Chem.* **314**, 2189 (2017).
84. R. Rajagopalan, S. Jain, A. Kaul, P. Trivedi. Biodistribution and pharmacokinetic studies on topicallydelivered technetium-99m-labeled 5-FU nanogel formulation for management of pre-cancerous skin lesions. *Tropical J. Pharmaceut. Res.* **18**, 1977 (2019).
85. M. Kubeil, Y. Suzuki, M. Casulli, R. Kamal, T. Hashimoto, M. Bachmann, T. Hayashita, H. Stephan. Exploring the potential of nanogels: from drug carriers to radiopharmaceutical agents. *Adv. Healthc. Mater.* **2023**, 2301404 (2023).
86. O. Estudiante-Mariquez, A. Rodríguez-Galván, D. Ramírez-Hernández, F. Contreras-Torres, L. Medina. Technetium-radiolabeled mannose-functionalized gold nanoparticles as nanoprobes for sentinel lymph node detection. *Molecules* **25**, 1982 (2020).
87. A. Walsh. Chemisorption of iodine-125 to gold nanoparticles allows for real-time quantitation and potential use in nanomedicine. *J. Nanopart. Res.* **19**, 152 (2017).
88. Q. Ng, C. Olariu, M. Yaffee, V. Taelman, N. Marincek, T. Krause, L. Meier, M. Walter. Indium-111 labeled gold nanoparticles for in-vivo molecular targeting. *Biomaterials* **35**, 7050 (2014).
89. E. Morales-Avila, G. Ferro-Flores, E. Ocampo-García, L. De Leon-Rodríguez, C. Santos-Cuevas, R. García-Becerra, L. Medina, L. Gomez-Olivan. Multimeric System of ^{99m}Tc-labeled gold nanoparticles conjugated to c[RGDfK(C)] for molecular imaging of tumor $\alpha(v)\beta(3)$ expression. *Bioconjug. Chem.* **22**, 913 (2011).

90. Y. Xing, J. Zhu, L. Zhao, Z. Xiong, Y. Li, S. Wu, G. Chand, X. Shi, J. Zhao. SPECT/CT imaging of chemotherapy-induced tumor apoptosis using ^{99m}Tc-labeled dendrimer-entrapped gold nanoparticles. *Drug Deliv.* **25**, 1384 (2018).
91. Y. Luo, L. Zhao, X. Li, J. Yang, L. Guo, G. Zhang, M. Shen, J. Zhao, X. Shi. The design of a multifunctional dendrimer-based nanoplatform for targeted dual mode SPECT/MR imaging of tumors. *J. Mater. Chem. B* **4**, 7220 (2016).
92. B. Murphy, A. Woodwick, K. Murphy, K. Chandler, G. Johnson, C. Hunt, P. Peller, J. Jakub, A. Homb. ^{99m}Tc-tilmanocept versus ^{99m}Tc-sulfur colloid in lymphoscintigraphy: sentinel lymph node identification and patient-reported pain. *J. Nucl. Med. Technol.* **47**, 300 (2019).
93. C. Santos, F. Filho, F. Campos, C. de Aguiar Ferreira, A. de Barros, D. Soares. Ag_2WO_4 nanoparticles radiolabeled with technetium-99m: a potential new tool for tumor identification and uptake. *J. Radioanal. Nucl. Chem.* **323**, 51 (2020).
94. D. El-Safoury, A. Ibrahim, D. El-Setouhy, O. Khowessah, M. Motaleb, T. Sakr. Gold nanoparticles for ^{99m}Tc-doxorubicin delivery: Formulation, in vitro characterization, comparative studies in vivo stability and biodistribution. *J. Radioanal. Nucl. Chem.* **328**, 325 (2021).
95. D. El-Safoury, A. Ibrahim, D. El-Setouhy, O. Khowessah, M. Motaleb, T. Sakr. Amelioration of tumor targeting and in vivo biodistribution of ^{99m}Tc-methotrexate-gold nanoparticles (^{99m}Tc-Mex-AuNPs). *J. Pharmaceut. Sci.* **110**, 2955 (2021).
96. A. Ashraf, R. Sharif, M. Ahmad, M. Masood, A. Shahid, D. Anjum, M. Rafique, S. Ghani. In vivo evaluation of the biodistribution of intravenously administered naked and functionalized silver nanoparticles in rabbit. *IET Nanobiotechnol.* **9**, 368 (2015).
97. P. Nallathamby, N. Mortensen, H. Palko, M. Malfatti, C. Smith, J. Sonnett, M. Doktycz, B. Gu, R. Roeder, W. Wang, S. Retterer. New surface radiolabeling schemes of super paramagnetic iron oxide nanoparticles (SPIONs) for biodistribution studies. *Nanoscale* **7**, 6545 (2015).
98. M. Nadeem, M. Ahmad, M. Saeed, A. Shaari, S. Riaz, S. Naseem, K. Rashid. Uptake and clearance analysis of Technetium99m labelled iron oxide nanoparticles in a rabbit brain. *IET Nanobiotechnol.* **9**, 136 (2015).
99. R. de Rosales, R. Tavaré, A. Glaria, G. Varma, A. Protti, P. Blower. ^{99m}Tc-bisphosphonate-iron oxide nanoparticle conjugates for dual-modality biomedical imaging. *Bioconjug. Chem.* **22**, 455 (2011).
100. I. Sandiford, A. Phinikaridou, A. Protti, L. Meszaros, X. Cui, Y. Yan, G. Frodsham, P. Williamson, N. Gaddum, R. Botnar, P. Blower, M. Green, R. de Rosales. Bisphosphonate-anchored PEGylation and radiolabeling of superparamagnetic iron oxide: long-circulating nanoparticles for in vivo multimodal (T1 MRI-SPECT) imaging. *ACS Nano* **7**, 500 (2013).
101. M. Motiei, T. Dreifuss, T. Sadan, N. Omer, T. Blumenfeld-Katzir, E. Fragogeorgi, G. Loudos, R. Popovtzer, N. Ben-Eliezer. Trimodal nanoparticle contrast agent for CT, MRI and SPECT imaging: Synthesis and characterization of radiolabeled core/shell iron oxide@gold nanoparticles. *Chem. Lett.* **48**, 291 (2019).
102. M. Mirković, M. Radović, D. Stanković, Z. Milanović, D. Janković, M. Matović, M. Jeremić, B. Antić, S. Vranješ-Đurić. ^{99m}Tc-bisphosphonate-coated magnetic nanoparticles as potential theranostic nanoagent. *Mater. Sci. Eng. C Mater. Biol. Appl.* **102**, 124 (2019).
103. F. Akhter, A. Rao, M. Abbasi, S. Wahocho, M. Mallah, H. Anees-ur-Rehman, Z. Chandio. A comprehensive review of synthesis, applications and future prospects for silica nanoparticles (SNPs). *Silicon* **14**, 8295 (2020).
104. F. Portilho, E. Helal-Neto, S. Cabezas, S. Pinto, S. Dos Santos, L. Pozzo, F. Sancenón, R. Martínez-Máñez, R. Santos-Oliveira. Magnetic core mesoporous silica nanoparticles doped with dacarbazine and labelled with ^{99m}Tc for early and differential detection of metastatic melanoma by single photon emission computed tomography. *Artif. Cells Nanomed. Biotechnol.* **46** (sup1), 1080 (2018).
105. A. de Barros, K. de Oliveira Ferraz, T. Dantas, G. Andrade, V. Cardoso, E. Sousa. Synthesis, characterization, and biodistribution studies of (99m)Tc-labeled SBA-16 mesoporous silica nanoparticles. *Mater. Sci. Eng. C Mater. Biol. Appl.* **56**, 181 (2015).
106. L. Pascual, F. Sancenón, R. Martínez-Máñez, T. Barja-Fidalgo, S. da Silva, A. de Jesus Sousa-Batista, C. Cerqueira-Coutinho, R. Santos-Oliveira. Mesoporous silica as multiple nanoparticles systems for inflammation imaging as nano-radiopharmaceuticals. *Micropor. Mesopor. Mater.* **239**, 426 (2017).
107. H. Gao, X. Liu, W. Tang, D. Niu, B. Zhou, H. Zhang, W. Liu, B. Gu, X. Zhou, Y. Zheng, Y. Sun, X. Jia, L. Zhou. 99mTc-conjugated manganese-based mesoporous silica nanoparticles for SPECT, pH-responsive MRI and anti-cancer drug delivery. *Nanoscale* **8**, 19573 (2016).
108. M. Tsuchimochi, K. Hayama, M. Toyama, L. Sasagawa, N. Tsubokawa. Dual-modality imaging with 99mTc and fluorescent indocyanine green using surface-modified silica nanoparticles for biopsy of the sentinel lymph node: An animal study. *EJNMMI Res.* **3**, 33 (2013).
109. A. Brouwers, D. De Jong, E. Dams, W. Oyen, O. Boerman, P. Laverman, T. Naber, G. Storm, F. Corstens. Tc-99m-PEG-liposomes for the evaluation of colitis in crohn's disease. *J. Drug Target* **8**, 225 (2000).
110. B. Goins, A. Bao, W. Phillips. Techniques for loading technetium-99m and rhenium-186/188 radionuclides into pre-formed liposomes for diagnostic imaging and radionuclide therapy. In: *Liposomes. Methods in Molecular Biology^{TM}*. Edited by V. Weissig (2010), Vol. 606.
111. P. Laverman, E. Dams, W. Oyen, G. Storm, E. Koenders, R. Prevost, J. van der Meer, F. Corstens, O. Boerman. A

novel method to label liposomes with 99mTc by the hydrazino nicotinyl derivative. *J. Nucl. Med.* **40**, 192 (1999).
112. B. Lasa-Saracíbar, S. El Moukhtari, T. Tsotakos, S. Xanthopoulos, G. Loudos, P. Bouziotis, M. Blanco-Prieto. In vivo biodistribution of edelfosine-loaded lipid nanoparticles radiolabeled with Technetium-99m: Comparison of administration routes in mice. *Eur. J. Pharm. Biopharm.* **175**, 1 (2022).
113. A. Ayan, A. Yenilmez, H. Eroglu. Evaluation of radiolabeled curcumin-loaded solid lipid nanoparticles usage as an imaging agent in liver-spleen scintigraphy. *Mater. Sci. Eng. C Mater. Biol. Appl.* **75**, 663 (2017).
114. V. Carmo, M. de Oliveira, L. Mota, L. Freire, R. Ferreira, V. Cardoso. Technetium-99m-labeled stealth pH-sensitive liposomes: a new strategy to identify infection in experimental model. *Braz. Arch. Biol. Technol.* **50**, 199 (2007).
115. M. Straub, M. Leresche, C. Pilloud, F. Devynck, N. Stritt, R. Hesselmann. A new two-strip TLC method for the quality control of technetium-99m mercaptoacetyl-triglycine (99mTc-MAG3). *EJNMMI Radiopharm. Chem.* **3**, 5 (2018).
116. P. Dubey, D. Singodia, R. Verma, S. Vyas. RGD Modified albumin nanospheres for tumour vasculature targeting. *J. Pharm. Pharmacol.* **63**, 33 (2011).
117. M. Marenco, L. Canziani, G. De Matteis, G. Cavenaghi, C. Aprile, L. Lodola. Chemical and physical characterisation of human serum albumin nanocolloids: Kinetics, strength and specificity of bonds with 99mTc and 68Ga. *Nanomaterials* **11**, 1776 (2021).
118. F. Blankenberg, J. Vanderheyden, H. Strauss, J. Tait. Radiolabeling of HYNIC-annexin V with technetium-99m for in vivo imaging of apoptosis. *Nat. Protoc.* **1**, 108 (2006).
119. Y. Yang, T. Neef, C. Mittelholzer, E. Garcia Garayoa, P. Bläuenstein, R. Schibli, U. Aebi, P. Burkhard. The biodistribution of self-assembling protein nanoparticles shows they are promising vaccine platforms. *J. Nanobiotechnol.* **11**, 36 (2013).
120. M. Liang, H. Tan, J. Zhou, T. Wang, D. Duan, K. Fan, J. He, D. Cheng, H. Shi, H. Choi, X. Yan. Bioengineered H-Ferritin nanocages for quantitative imaging of vulnerable plaques in atherosclerosis. *ACS Nano* **12**, 9300 (2018).
121. C. Aprile, L. Lodola. A narrative review of ^{99m}Tc-aprotinin in the diagnosis of cardiac amyloidosis and a new life for an unfairly abandoned drug. *Biomedicines* **10**, 1377 (2022).
122. V. Pandeya, T. Haidera, A. Chandak, A. Chakraborty, S. Banerjee, V. Sonia. Technetium labeled doxorubicin loaded silk fibroin nanoparticles: Optimization, characterization and in vitro evaluation. *J. Drug Deliv. Sci. Technol.* **56**, 101539 (2020).
123. L. Kovacs, M. Tassano, M. Cabrera, M. Fernández, W. Porcal, R. Anjos, P. Cabral. Labeling polyamidoamine (PAMAM) dendrimers with technetium-99m via hydrazinonicotinamide (HYNIC). *Curr. Radiopharm.* **7**, 115 (2014).
124. H. Agashe, A. Babbar, S. Jain, R. Sharma, A. Mishra, A. Asthana, M. Garg, T. Dutta, N. Jain. Investigations on biodistribution of technetium-99m-labeled carbohydrate-coated poly(propylene imine) dendrimers. *Nanomedicine: Nanotechnol. Biol. Med.* **3**, 120 (2007).
125. A. Ebrahimi, M. Pirali Hamedani, P. Mohammadzadeh, M. Safari, S. Esmaeil Sadat Ebrahimi, M. Seyed Hamzeh, M. Shafiee Ardestani, S. Masoumeh Ghoreishi. ^{99m}Tc-anionic dendrimer targeted vascular endothelial growth factor as a novel nano-radiotracer for in-vivo breast cancer imaging. *Bioorg. Chem.* **128**, 106085 (2022).
126. N. Mohtavinejad, M. Amanlou, A. Bitarafan-Rajabi, A. Khalaj, A. Pormohammad, M. Ardestani. Technetium-99m-PEGylated dendrimer-G2-(Dabcyle-Lys6,Phe7)-pHBSP: A novel nano-radiotracer for molecular and early detecting of cardiac ischemic region. *Bioorg. Chem.* **98**, 103731 (2020).
127. L. Porto, D. Silva, A. de Oliveira, A. Pereira, K. Borges. Carbon nanomaterials: synthesis and applications to development of electrochemical sensors in determination of drugs and compounds of clinical interest. *Rev. Anal. Chem.* **38**, 20190017 (2019).
128. C. Zhao, J. Kang, Y. Li, Y. Wang, X. Tang, Z. Jiang. Carbon-based stimuli-responsive nanomaterials: classification and application. *Cyborg Bionic Syst.* **4**, 0022 (2023).
129. K. Soumya, N. More, M. Choppadandi, D. Aishwarya, G. Singh, G. Kapusetti. A comprehensive review on carbon quantum dots as an effective photosensitizer and drug delivery system for cancer treatment. *Biomed. Technol.* **4**, 11 (2023).
130. K. Naik, S. Chaudhary, L. Ye, A. Parmar. A strategic review on carbon quantum dots for cancer-diagnostics and treatment. *Front. Bioeng. Biotechnol.* **10**, 882100 (2022).
131. E. Castro, A. Hernandez Garcia, G. Zavala, L. Echegoyen. Fullerenes in biology and medicine. *J. Mater. Chem B* **5**, 6523 (2017).
132. N. Bayoumi, A. Emam. ^{99m}Tc radiolabeling of polyethylenimine capped carbon dots for tumor targeting: synthesis, characterization and biodistribution. *Int. J. Radiat. Biol.* **97**, 977 (2021).
133. E. Gharepapagh, A. Fakhari, T. Firuzyar, A. Shomalid, F. Azimie. Preparation, biodistribution and dosimetry study of Tc-99m labeled N-doped graphene quantum dot nanoparticles as a multimodular radiolabeling agent. *New J. Chem.* **45**, 3909 (2021).
134. S. Ghoreishi, A. Najdian, S. Yadegari, M. Seyedhamzeh, M. Etemadzade, M. Mirzaei, S. Hadadian, Z. Alikhani, M. Ardestani. The use of carbon quantum dot as alternative of stannous chloride application in radiopharmaceutical kits. *Contrast Media Mol. Imaging.* **2020**, 4742158 (2020).
135. M. Roeinfard, M. Zahedifar, M. Darroudi, K. Sadri, A. Zak. Preparation of technetium labeled-graphene quantum dots and investigation of their bio distribution. *J. Cluster Sci.* **33**, 1 (2022).

136. M. Bastos, M. Pijeira, J. de Souza Sobrinho, A. Dos Santos Matos, E. Ricci-Junior, P. de Almeida Fechine, L. Alencar, S. Gemini-Piperni, F. Alexis, M. Attia, R. Santos-Oliveira. Radiopharmacokinetics of graphene quantum dots nanoparticles in vivo: Comparing the pharmacokinetics parameters in long and short periods. *Curr. Top Med. Chem.* **22**, 2527 (2022).
137. F. de Menezes, S. Dos Reis, S. Pinto, F. Portilho, F. do Vale Chaves, E. Mello, E. Helal-Neto, A. da Silva de Barros, L. Alencar, A. de Menezes, C. Dos Santos, A. Saraiva-Souza, J. Perini, D. Machado, I. Felzenswalb, C. Araujo-Lima, A. Sukhanova, I. Nabiev, R. Santos-Oliveira. Graphene quantum dots unraveling: green synthesis, characterization, radiolabeling with ^{99m}Tc, in vivo behavior and mutagenicity. *Mater. Sci. Eng. C Mater. Biol. Appl.* **102**, 405 (2019).
138. L. Ruili, D. Qianqian, S. Xiaoguang, C. Shaoliang, L. Wenxin. Biodistribution of fullerene derivative $C_{60}(OH)_x(O)_y$. *Chin. Sci. Bull.* **46**, 615 (2001).
139. L. Qingnuan, X. yan, Z. Xiaodong, L. Ruili, D. Qieqie, S. Xiaoguang, C. Shaoliang, L. Wenxin. Preparation of (99m)Tc-C(60)(OH)(x) and its biodistribution studies. *Nucl. Med. Biol.* **29**, 707 (2002).
140. D. Cagle, S. Kennel, S. Mirzadeh, J. Alford, L. Wilson. In vivo studies of fullerene-based materials using endohedral metallofullerene radiotracers. *Proc. Natl. Acad. Sci. USA* **96**, 5182 (1999).
141. L. Karam, M. Mitch, B. Coursey. Encapsulation of ^{99m}Tc within fullerenes: a novel radionuclidic carrier. *Appl. Rad. Isotopes.* **48**, 771(1997).
142. W. Burch, P. Sullivan, C. McLaren. Technegas – a new ventilation agent for lung scanning. *Nucl. Med. Commun.* **7**, 865 (1986).
143. D. Mackey, W. Burch, I. Dance, K. Fisher, G. Willett. The observation of fullerenes in a Technegas lung ventilation unit. *Nucl. Med. Commun.* **15**, 430 (1994).
144. P. Le Roux, W. Schafer, F. Blanc-Beguin, M. Tulchinsky. Ventilation scintigraphy with radiolabeled carbon nanoparticulate aerosol (Technegas): state-of-the-art review and diagnostic applications to pulmonary embolism during COVID-19 pandemic. *Clin. Nucl. Med.* **48**, 8 (2023).
145. P. Jackson, R. Baker, D. McCulloch, D. Mackey, H. van der Wall, G. Willett. A study of Technegas employing X-ray photoelectron spectroscopy, scanning transmission electron microscopy and wet-chemical methods. *Nucl. Med. Commun.* **17**, 504 (1996).
146. T. Senden, K. Moock, J. Gerald, W. Burch, R. Browitt, C. Ling, G. Heath. The physical and chemical nature of technegas. *J. Nucl. Med.* **38**, 1327 (1997).
147. C. Liao, Y. Li, S. Tjong. Graphene nanomaterials: synthesis, biocompatibility, and cytotoxicity. *Int. J. Mol. Sci.* **19**, 3564 (2018).
148. W. Jeong, H. Choi, K. Kim. Graphene-based nanomaterials as drug delivery carriers. *Adv. Exp. Med. Biol.* **1351**, 109 (2022).
149. S. Challan, A. Massoud. Radiolabeling of graphene oxide by Technetium-99m for infection imaging in rats. *J. Radioanal. Nucl. Chem.* **314**, 2189 (2017).
150. J. Da-wei, P. Cheng, S. Yan-Hong, J. Li-Na, L. Jian-Bo, Z. Lan. Study on technetium-99m labeling of graphene oxide nanosheets through click chemistry-Tc-99m labeling of graphene oxide nanosheets. *Nucl. Sci. Tech.* **26**, 1001 (2015).
151. A. Sasidharan, S. Swaroop, C. Koduri, C. Girish, P. Chandran, L. Panchakarla, V. Somasundaram, G. Gowd, S. Nair, M. Koyakutty. Comparative in vivo toxicity, organ biodistribution and immune response of pristine, carboxylated and PEGylated few-layer graphene sheets in Swiss albino mice: A three month study. *Carbon* **95**, 511 (2015).
152. Y.-J. Lu, C. Lin, H. Yang, K.-J. Lin, S.-P. Wey, C.-L. Sun, K.-C. Wei, T.-C. Yen, C. Lin, C. Ma, J.-P. Chen. Biodistribution of PEGylated graphene oxide nanoribbons and their application in cancer chemo-photothermal therapy. *Carbon* **74**, 83 (2014).
153. F. Yurt, O. Ersöz, E. Harputlu, K. Ocakoglu. Preparation and evaluation of effect on Escherichia coli and Staphylococcus aureus of radiolabeled ampicillin-loaded graphene oxide nanoflakes. *Chem. Biol. Drug Des.* **91**, 1094 (2019).
154. S. Rathinavel, K. Priyadharshini, D. Panda. A review on carbon nanotube: An overview of synthesis, properties, functionalization, characterization, and the application. *Mater. Sci. Engineer. B* **268**, 115095 (2021).
155. R. Reilly. Carbon nanotubes: Potential benefits and risks of nanotechnology in nuclear medicine. *J. Nucl. Med.* **48**, 1039 (2007).
156. S. Datir, M. Das, R. Singh, S. Jain. Hyaluronate tethered, "smart" multiwalled carbon nanotubes for tumor-targeted delivery of doxorubicin. *Bioconjug. Chem.* **23**, 2201 (2012).
157. J. Wang, L. Cabana, M. Bourgognon, H. Kafa, A. Protti, K. Venner, A. Shah, J. Sosabowski, S. Mather, A. Roig, X. Ke, G. Tendeloo, R. de Rosales, G. Tobias, K. Al-Jamal. Magnetically decorated multi-walled carbon nanotubes as dual MRI and SPECT contrast agents. *Adv. Funct. Mater.* **24**, 1880 (2014).
158. J. de Alcantara Lemos, D. Soares, N. Pereira, L. Gomides, J. de Oliveira Silva, G. Bruch, G. Cassali, L. Alisaraie, R. Alves, A. Santos, A. de Barros. Preclinical evaluation of PEG-Multiwalled carbon nanotubes: Radiolabeling, biodistribution and toxicity in mice. *J. Drug Deliv. Sci. Technol.* **86**, 104607 (2023).
159. Y. Du, Z. Chen, M. Hussain, P. Yan, C. Zhang, Y. Fan, L. Kang, R. Wang, J. Zhang, X. Ren, C. Ge. Evaluation of cytotoxicity and biodistribution of mesoporous carbon nanotubes (pristine/-OH/-COOH) to HepG2 cells in vitro and healthy mice in vivo. *Nanotoxicology* **16**, 895 (2002).
160. Q. Wei, L. Zhan, B. Juanjuan, W. Jing, W. Jianjun, S. Taoli, G. Yi'an, W. Wangsuo. Biodistribution of co-exposure to multi-walled carbon nanotubes and nanodiamonds in mice. *Nanoscale Res Lett.* **7**, 473 (2012).

161. R. Fernandesa, J. Lemos, A. de Barros, V. Geraldo, E. da Silva, L. Alisaraie, D. Soares. Carboxylated versus bisphosphonate SWCNT: functionalization effects on the biocompatibility and in vivo behaviors in tumor-bearing mice. *J. Drug Deliv. Sci. Technol.* **50**, 266 (2019).

Received 20.06.24

В. Трусова, І. Карнаухов, А. Зелінський,
Б. Борц, І. Ушаков, Л. Сиденко, Г. Горбенко

ТЕХНЕЦІЙ-99м: НОВИЙ ПОГЛЯД
З ТОЧКИ ЗОРУ НАНОМАТЕРІАЛІВ

Радіомаркування наноматеріалів за допомогою технецію-99м (^{99m}Tc) виокремилося як перспективна стратегія, що інтегрує переваги нанотехнологій та ядерної медицини для діагностичних та терапевтичних застосувань. Дана робота має на меті надати всебічний огляд сучасного стану у сфері радіомаркування наноматеріалів за допомогою ^{99m}Tc. Дослідження охоплює методи синтезу, механізми маркування, біологічні застосування, фізико-хімічні характеристики та клінічні застосування наноматеріалів, мічених ^{99m}Tc. Розглядаються різноманітні категорії наноматеріалів, включно з органічними та неорганічними наночастинками, ліпідними та білковими наносистемами, а також різними карбоновими наноматеріалами. Крім того, в огляді звернено увагу на виклики, притаманні цій галузі, такі як стабільність радіомітки, потенційна токсичність наноматеріалів та регуляторні аспекти. Обговорено також перспективні напрямки для розвитку досліджень у сфері наноматеріалів, мічених ^{99m}Tc.

Ключові слова: наноматеріали, терагностика, технецій, наномедицина, радіомаркування.